Delft University of Technology
Department of Applied Earth Sciences

MASTER'S THESIS

A Structural Modeling Approach on Timing & Evolution of Mesozoic Anticlines in the Western High Atlas, Morocco.

Petroleum Engineering & Geosciences

Author:
Christian Kluge (4421094)

to obtain the degree of Master of Science,
defended publicly on the 8th of July, 2016 at 13:30.

Supervisors:
Prof. Dr. Giovanni Bertotti
Msc. Rémi Charton

Committee members:
Dr. Joep Storms
Msc. Lisanne Douma

July 8, 2016

Thesis title:	"A Structural Modeling Approach on Timing & Evolution of Mesozoic Anticlines in the Western High Atlas, Morocco."

Keywords:	Morocco, Western High Atlas, Structural Modeling, Salt Diapirism, Basin Geology

Author(s):	Christian Kluge
Professor(s):	Prof. Dr. Giovanni Bertotti
Supervisor(s):	Prof. Dr. Giovanni Bertotti Msc. Rémi Charton
Committee:	Prof. Dr. Giovanni Bertotti (Applied Geology) Dr. Joep Storms (Applied Geology) Msc. Rémi Charton (Applied Geology) Msc. Lisanne Douma (Applied Geophysics)
Postal Address:	Section for Applied Geology Department of Geoscience & Engineering Faculty of Civil Engineering & Geosciences Delft University of Technology P.O. Box 5028 The Netherlands
Telephone:	(31) 15 2781328 (secretary)
Telefax:	(31) 15 2781189

Acknowledgements

Many thanks to Prof. Dr. Giovanni Bertotti for always guiding and inspiring me during the thesis, as well as being a great supervisor who was always available to give support. I would also like to thank Rémi Charton as my second supervisor, always providing the opportunity for constructive geological discussions, as well as Dr. Joep Storms and Lisanne Douma (TU Delft) for being the third and fourth committee member for my thesis defence.

Without Aude Duval-Arnould (NARG) from the University of Manchster, I wouldn't have had the possibility to go on a field trip to study the two anticlines that are part of both of our projects. I am thankful to her and Dr. Stefan Schröder (NARG), her supervisor, for allowing me to use and share all the data and observations that we made in field, although the field trip only intended to support her project.

I am particularly grateful for the assistance with *3D Move* given by Jan-Kees Blom (TU Delft), and Kevin Bisdom (TU Delft) for introducing me to the *Gocad* applications. Thanks also to Max Holicki (TU Delft) for supporting me with his *Matlab* skills. Barnaby Fryer has always been a great study companion from the first day and he helped me with checking the spelling and grammar.

Ultimately, I would like to thank my parents for providing me with the possibility of studying abroad and their all time motivational support throughout my academic career. For the emotional and mental support I would like to thank my girlfriend, Mi.

Delft - July 8, 2016

Christian Kluge

TU Delft Delft University of Technology

North Africa Research Group
www.narg.org.uk

Abstract

The Moroccan passive margin has been the objective of a variety of studies to investigate the petroleum potential and to locate play systems in the offshore and partly onshore Agadir-Essaouira basin. These basins are largely dependent on the structural development of Atlas mountains, being characterised by different phases of tectonic rifting, regional shortening and differential exhumation and subsidence patterns. The evolution of salt-cored anticlines in the Western High Atlas are possibly a key in understanding the tectonic history of the area especially in the context of the observed vertical movements.

This study has the aim to provide additional information on timing and evolution of salt-cored anticlines in the Western High Atlas, to get a better understating of folding mechanisms related to vertical movements in the hinterland. Their role in controlling sedimentation pathways is investigated, since the basin links the paleozoic massifs as a sediment source and the offshore as sediment sink system. A new modeling technique was applied to two salt-cored anticlines, the Jbel Amsittene and the Imouzzer anticline, combining remote sensing geological and structural data, integrated in a 3D structural modeling environment (Gocad). This allows for the extraction of the thickness distribution for the identification of pre-Alpine locations of sediment depocenters. Further, the tectonic history of folding, using 2D section balancing (Move) and 3D unfolding and strain analysis (Gocad), is investigated. In a small field study, the large scale modeling results are compared to small scale field observations. Salt and folding mechanisms in the context of the geological setting and history are discussed and their impact on Jurassic to Early Cretaceous sediment pathways are outlined. The expression of folding on the sea-floor and the impact of the presence of pre-orogenic anticlines on the Alpine folding processes are debated.

The results suggest Early to Middle Jurassic salt activities potentially initiated by pre-orogenic exhumation in the hinterland and subsidence towards the offshore, resulting in a hydraulic head gradient causing salt flow. Another scenario are pre-orogenic phases of tectonic shortening or salt flow by increased thermal activities. The topography that was created certainly controlled the sediment distribution of passive margin sands into the offshore basin. Jurassic salt mobilisation also had an impact on the Alpine-folding process which might have resulted in a connection of smaller isolated salt diapirs leading to a variety of strike orientations of folds in the basins.

Contents

List of Figures

1 Introduction

Morocco has been a target of fossil resource exploration companies for many years. Still, only two petroleum systems have been documented in the onhsore Essaouira basin with small producing oil and gas fields [42]. New reservoirs are now aimed for in the offshore areas in the Agadir-Essaouira basin. The distribution of submarine fans, mainly clastic reservoirs, play a key role in understanding the reservoir distribution in the deep sea. One example is given by the Tan-Tan Delta, a large deep sea fan in offshore Agadir [29], which probably formed due to the channelisation of passive margin sands from the Reguibat shield. Mechanisms like these are also likely to have occurred north of Agadir, in the Western High Atlas, which is under recent scientific discussion from scientists of the North Africa Research Group (NARG) based in Manchester. NARG is trying to predict the distribution of offshore reservoirs by investigating folding processes onshore and offshore, examining the evidence of erosional surfaces, studying the carbonate reef distribution in outcrops and qualifying and quantifying vertical movements.

Therefore, this thesis aims to provide additional information on whether sediment distribution is controlled by larger folds forming during the Jurassic to Cretaceous, possibly linked to vertical movements along the passive margin, prior to the Late Cretaceous to Neogene Alpine orogeny. If those folds were forming a topography in the Jurassic to Early Cretaceous, they have an essential impact on sediment distribution in the present day offshore. This raises questions about the fold expression on the sea-floor, and, further, if folds have been present in pre-orogenic stages, what was their impact on folding process in the Alpine orogeny?

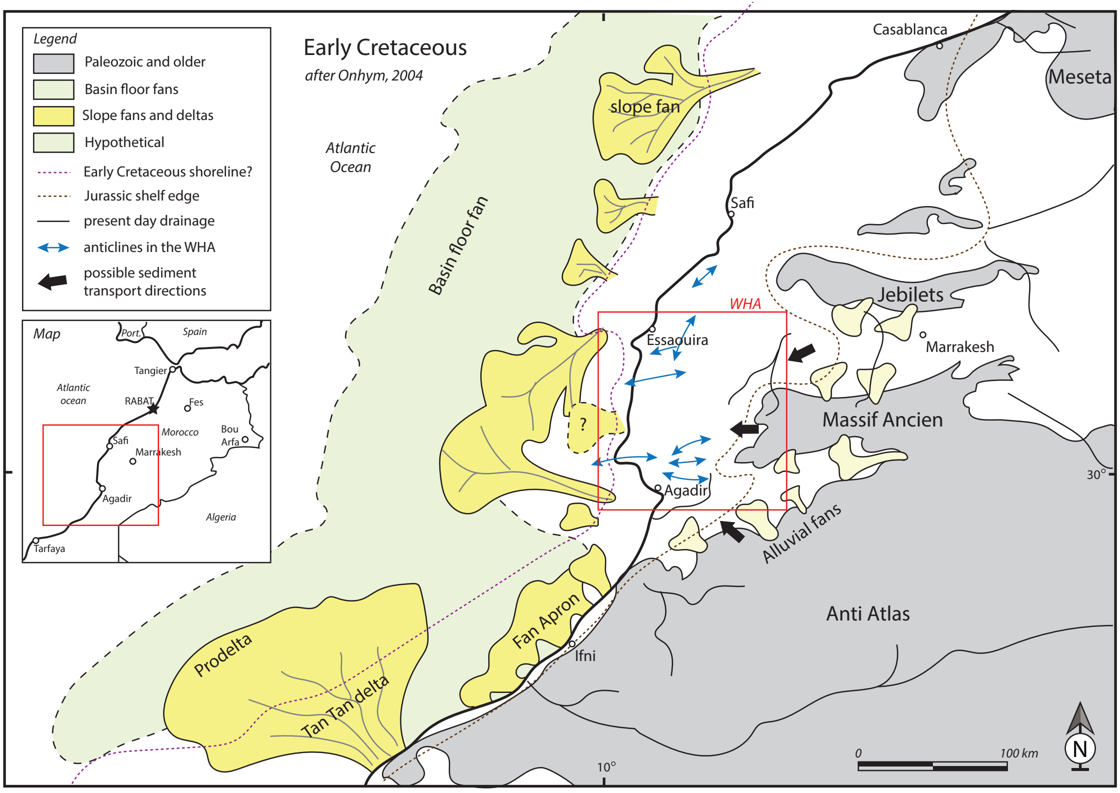

Figure 1: *Assumed offshore fans and their dependence on onshore anticlines in WHA (after Onhym, 2004).*

To investigate these hypotheses, two folds were analysed in terms of (1) thickness distributions in a 3D geological model that might indicate pre-orogenic fold patterns or diapiric activities, (2) process-based modeling to demonstrate possible tectonic signals throughout the Jurassic and Early Cretaceous and to analyse strain, and (3) geological features suggesting syn-sedimentary fold growth. The two anticlines are the Jbel Amsittene anticline in the northern part of the Western High Atlas and the Imouzzer anticline in the southern part (fig. 2). Both have a slightly different morphology and stratigraphy and are therefore interesting to test the above mentioned theories to either find differences or similarities in the evolution of these folds.

The first chapters of this thesis provide information about the geological background in the Western High Atlas, to provide a clear understanding of the tectonic evolution of the area. The importance of fault networks on salt diapirism in the onshore and offshore area is emphasised here. The stratigraphy of the area is shortly described to explain the influence of different rock types on fold growth or salt mobilisation. Data sources and selection show how the data was gathered from remote sensing and field study analysis. Thereafter, the approaches and techniques to build a 3D structural model are outlined. Observations and results from the modeling and field work are shown and discussed in terms of possible structural evolution scenarios for the two anticlines based on the results and their role in controlling sediment distribution in the Western High Atlas towards the offshore.

2 Geological Setting

2.1 Tectonic Setting

The Atlas system is an active orogenic fold-belt system, located in the northwestern part of Africa, extending over some 2000km from offshore Agadir in the west and continues onshore in ENE direction traversing Morocco, Algeria, and eventually reaching Tunisia [5], [13], [21], [29]. The mountain belt can be subdivided into several massifs and basins that follow different uplift and subsidence histories, as well as different periods of extension and compression from Paleozoic to present. The Moroccan Atlas mountains are subdivided into the Middle Atlas (MA) and the High Atlas (HA), where is HA is again subdivided into the Central and Eastern High Atlas (CEHA) and the Western High Atlas (WHA). The area of interest of this study is the Western High Atlas (WHA) bounded by the High Atlas (or Massif Ancien) in the west, the Meseta to the north, the Souss Basin in the south and the offshore basin to the east.

The Variscan belt, formed during the NNE compressional Hercynian orogeny that merged Laurussia and Gondwana to the supercontinent of Pangea, extends into the Meseta and Anti-Atlas domains, where they are widely exposed in large Paleozoic massifs. Their evolution was accompanied by significant metamorphism and magmatic intrusions [29]. The orogeny is characterised by the inhomogeneous nature of deformation, usually concentrated in elongate and narrow shear zones that acted as weakness zones by the end of the Paleozoic [35]. The Precambrian and Paleozic basement, being composed of metamorphic rocks and granitoids topped by late Precambrian volcanics, crops out in several Massifs, such as the Jebilet Massif, the Western High Atlas and the Anti-Atlas in the south [13]. The massifs provided large amounts of sediment during phases of exhumation and erosion.

During the early stages of the Mesozoic, the High Atlas domain experienced extension and rifting, first during the Triassic, as recorded by red beds and tholeiitic basalts, and later during the Jurassic, with the deposition of marine carbonates and shales capped by continental red beds [45]. The break-up of Pangea is expressed by successive extensional episodes in an overall rifting context, generally trending in a NE-SW direction [14],[29]. It represents an almost symmetrical oceanic basin with two conjugate margins of North America and northwest Africa to western Europe [47]. The onset of spreading in the Central Atlantic domain is not very well constrained and is only based on Middle Aalenian to Bajoian sediment lying unconformably on basalts on the Canary Islands [29], dated to Late Jurassic to recent [46]. The extensional syn-rift structures are N-S to NNE-SSW orientated and segmented by east-west transform faults [21]. The location of the WHA segment is most special since it connects the High Atlas fold belt intercepting the Atlantic passive margin [29]. Rifting is assumed to have ended at around 170-145 Ma in the northern parts and 150-135 Ma in the southern parts of the High Atlas [17].

From the Late Cretaceous onwards, the collision between Africa and Europe, the Alpine inversion, caused a NNW-SSE-directed compression [21]. The present-day structure is dominated by thick-skinned thrusting and folding, essentially by inversion of Mesozoic extensional faults and by buckling of both pre-Mesozoic basement and its sedimentary cover [45]. The main tectonic event creating the present-day topography occurred during late Miocene to Pliocene time [14].

2.2 Stratigraphy of the Mesozoic

The Mesozoic successions that are targeted in this study crop out almost exclusively in the Central High Atlas and the Atlantic basin south of Essaouira. The total thickness of the post-Hercynian sediments in the Essaouira basin range from 2 to 6.5 km [14]. A stratigraphic column combining observations from recent studies in the NARG project, as well as observations from the field study, is shown in figure 3. A geological map of the WHA is shown in figure 2 [10].

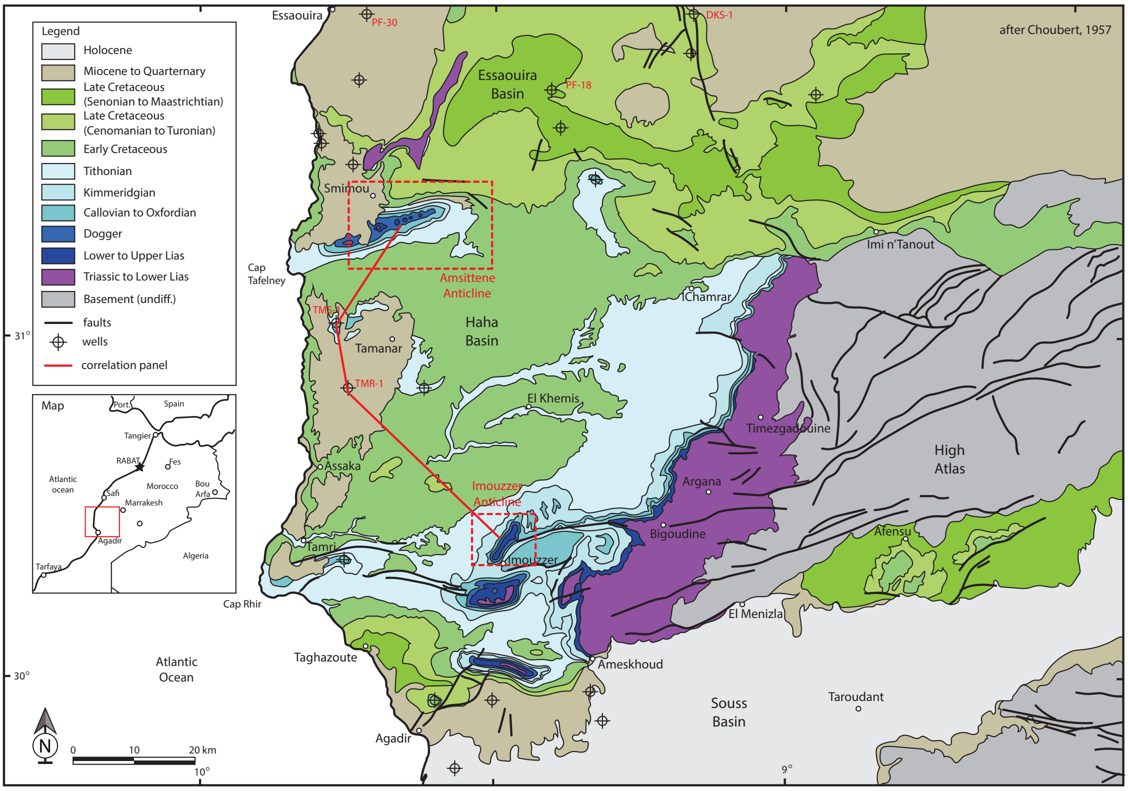

Figure 2: *Geological map of the Western High Atlas showing the studied anticlines (after Choubert, 1957).*

Triassic

Triassic rocks are mainly cropping out along the Argana Valley where they form 2500 to 5000m thick deposits of Lower Triassic sandstones, clays, mudstones and dolomites covered by Middle and Late Triassic carbonates and evaporites grading eastwards to marine carbonates [7], [13], [35]. They unconformably rest on Lower Paleozoic beds or directly on the Precambrian basement giving evidence for strong Triassic erosion [7], [13], [30]. Two main intercalated volcanic horizons are forming very strong seismic markers in the fluvio-lacustrine domain [14] can be referred to as tholeiitic basalt flows of the Central Atlantic Magmatic Province (CAMP) with absolute ages ranging from 197-208 Ma [29]. Basin salts are commonly intercalated or deposited on top of Triassic sequences [20], [21], [42].

Jurassic

Lower Liassic carbonates indicate the return of carbonate sedimentation from the south-west, induced by transgression[13], [17]. In the Late Early to early Middle Jurassic, open marine deposition established on the Moroccan continental margin creating depositional environments ranging from carbonate ramps to deltas [13]. Reddish salts were documented in the Anklout anticline in the southern vicinity of the Imouzzer anticline in the Lias inf. [1]. The Middle Jurassic (Dogger), regression resulted in the first post-rift deposition [14], which was composed of thick conglomerates, sand- and siltstones with thicknesses of 200-400m in the west, diminishing to 10-70m in the east, where fluvial deposition took place [13]. In the northern parts of the basin, these deposits are almost exclusively carbonatic and dolomitic limestones.

In the Late Jurassic (Malm), a Callovian flooding surface marks the installation of a carbonate platform [29]. Other authors suggest that this massive and widespread Jurassic carbonate platform dominated the earliest post-rift phase [13] and was interrupted by influx of siliclasitics as a result of a poorly understood basin-wide regressional episode [42]. Rimmed carbonate shelves and homoclinal ramps, as well as thin intra-shelf platforms and local sand bars developped throughout the Mid-Oxfordian showing no continuous linear reef trend [47]. The Late Oxfordian to Early Kimmeridgian comprises mud-/wackestones, bioturbated carbonates and dolomites thickenning from NE to SW, later showing strong terrigenous influx leading to sandstone, marl, evaporite and dolomite deposition making the Kimmeridgian clearly detectable by its red marls in the western part of the basin [47]. Late Kimmeridgian to Tithonian deposition is again replaced by carbonate-evaporites in shallow marine to supratidal environments [47]. The stratigraphic record reflects the combined effects of tectonic pulsations (rifting episodes) and climate changes on sedimentation [29].

Cretaceous

The Lower Cretaceous sedimentation developed over an almost general unconformity, which signals erosion and marks a complete change of sedimentary environment, and is now dominated by alluvial plains and siliciclastic facies [29]. This was a result of the Early Cretaceous lowering of sea-level, which lead to clastic deposition in the basin (e.g. Tan-Tan Delta) and consequently to some diapiric growth in the inboard part of the basin [42]. The uplift of the WMA [21] is seen as source of Lower Cretaceous turbidites in the Atlantic margin and a narrow gulf in the Essaouira basin, i.e. the North High Atlas Gulf in the Valangian to Aptian as described by Michard et al. (2008) [29]. These observations are in good agreement with the logs taken by Züehlke et al. (2004), in which sandy intervals were described in the Hautervian to Aptian [47]. Some latest observation from the NARG group confirmed the existence of a 40m thick sand interval outcropping near Assaka which is assumed to be a major reservoir sequence in the offshore. Pre-Alpine deformation of these sediments is assumed to be only influenced by salt tectonics [21]. In the Upper Cretaceous (Cenomanian and Turonian), a major transgression was marked by deposition of limestones [14]. At the time, the coastline shifted some 100km to the east [42].

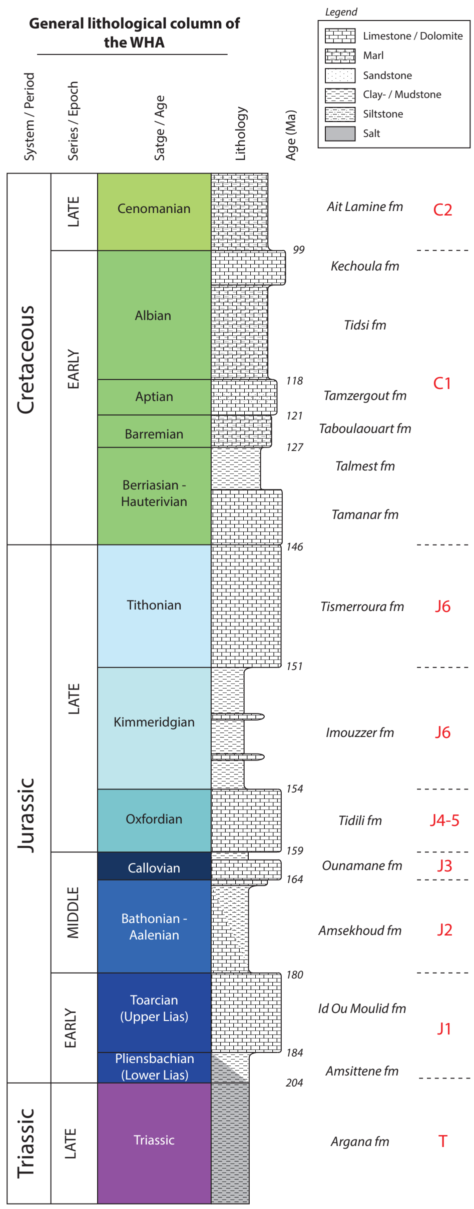

Figure 3: *Lithological column in the Haha basin (after Choubert, 1957 & Aude Duval-Arnould (NARG)).*

2.3 Faulting, Folding & Diapirism

To better understand the structural evolution of the study area, it is important to understand the fault and fold systems, as well as the role of salt diapirism. Hafid et al. (2000), emphasised the importance of pre-existing fault systems that were reactivated and inversed during the respective rifting and compressional stages [20]. The Eastern Diapiric Provinces extends over some 900km in the area and highly affected the structural setting in the WHA [29].

Faulting and Folding

This Early Triassic extensional fault regime of the Atlantic describes the reactivation of Hercynian fault sytems [17] and can be considered responsible for the location of the Triassic (salt) basins formed in a NW-SE tensional field [45]. The basin records strong subsidence from Triassic to Liassic time and a lesser pulse of subsidence during the Malm [14]. In onshore basins, the structures of the Moroccan margin are bounded by northerly striking faults and their halfgrabens, filled with at least 2000m of continental red beds overlain by basalt flows and silts [29]. Normal faulting ceased before the Liassic (at around 196 Ma), which coincides with or is significantly older than the appearance of oceanic crust in the Central Atlantic [5]. Later, during Jurassic and Cretaceous times, the Essaouira-Agadir domain was fragmented by several transcurrent faults, which triggered and enhanced diapiric ascent [34]. The Alpine inversion changes the tectonic and structural setting from the Late Cretaceous once again to a generally N-S compressional system which formed the present day topography of the High Atlas mountains [29]. This compression resulted in reverse faulting, inversion of selected Triassic to Jurassic syn-rift structures and evaporite-based detachment folding [21].

Diapirism

The Eastern Diapiric Province stronlgy influenced the post-rift sedimentary and structural evolution of onshore and offshore Essaouira basin [29]. Salt deposition occurred on top of, or in lateral facies transition of continental to coastal Triassic sedimentary sequences in syn-rift half-grabens [21], [42], but mainly in the transitional phase between rifting and drifting [20]. The amount of salt varies along the margin along strike, which can be mainly attributed to the underlying syn-rift basement structure that determined the initial configuration of the salt-bearing sub-basins [42]. Further, the variable distribution of evaporites from post-Triassic processes could have resulted from a combination of (1) extrusion to the sea floor and sea-water dissolution, (2) extrusion and hydrothermal dissolution and (3) extrusion during Cenozoic diapir rejuvenation or surficial dissolution during Tertiary uplift and exhumation of the Central High Atlas [39].

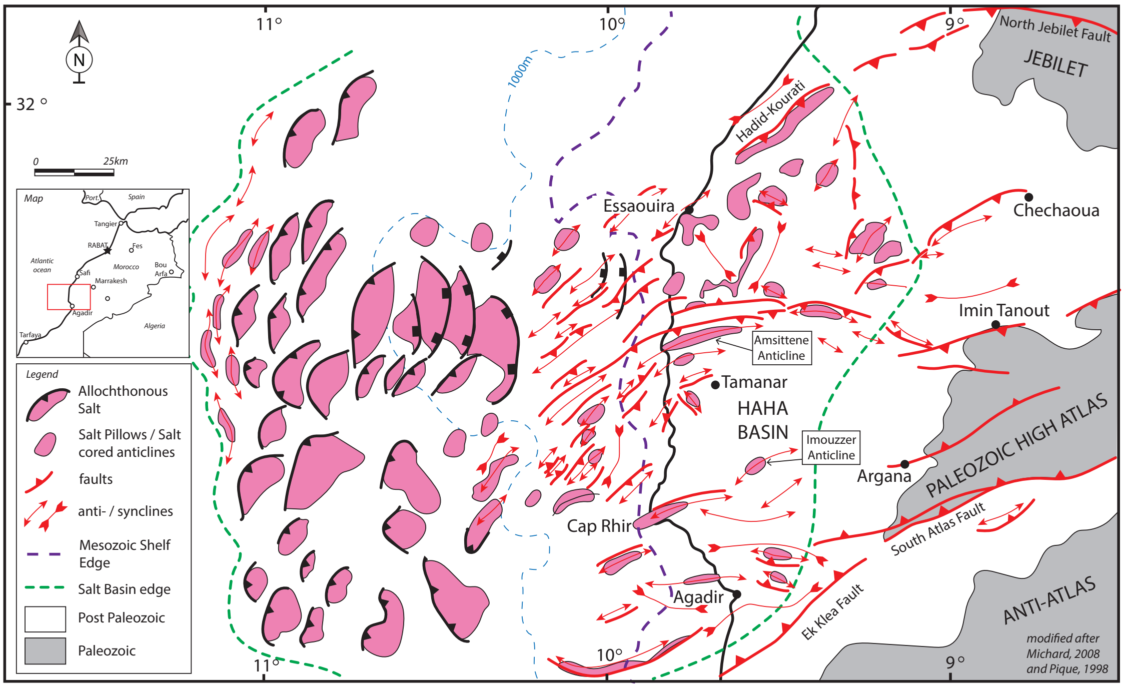

Figure 4: *Map of the offshore and Western High Atlas salt basin (after Michard, 2008 and Piqué, 1998).*

Salt mobilisation and deformation is assumed to have taken place in various stages initiated by different mechanisms, which makes this salt province complex and diffuse. The Triassic to Lower Liassic salt layers were mobilised shortly after deposition [29] and later triggered by the Late Jurassic thermal subsidence during the post-rift evolution of the margin [42]. Hafid et al. (2006) described some Early Cretaceous deformations of sediments only linked to salt tectonics, although the extensional movements had already ceased. Further, the Late Eocene and subsequent Miocene inversional episodes reactivated the pre-existing salt structures along the margin and appear to be the main period of forming salt sheets and canopies offshore [42]. The gravity potential in the study area is provided by the differential uplift of the Atlas mountains perpendicular to the margin, which caused the salt diapirs to migrate from proximal to distal, or east to west, of the margin [21], [42].

2.4 Vertical Movements in the Moroccan Passive Margin

Vertical movements of the continental crust and related changes of topography are the consequence of a wide variety of processes, such as thermal uplift or subsidence, lithospheric folding, tectonic inversion, mantle up- or down welling, and crustal shortening [11]. Recent studies make use of low temperature geochronology that can be used to determine the vertical movement of a stratigraphic sequence throughout geological time. They revealed the existence of major tectonic vertical motions that affected large domains on the eastern margin of the Central Atlantic Ocean by the Middle Jurassic (fig. 5) [19].

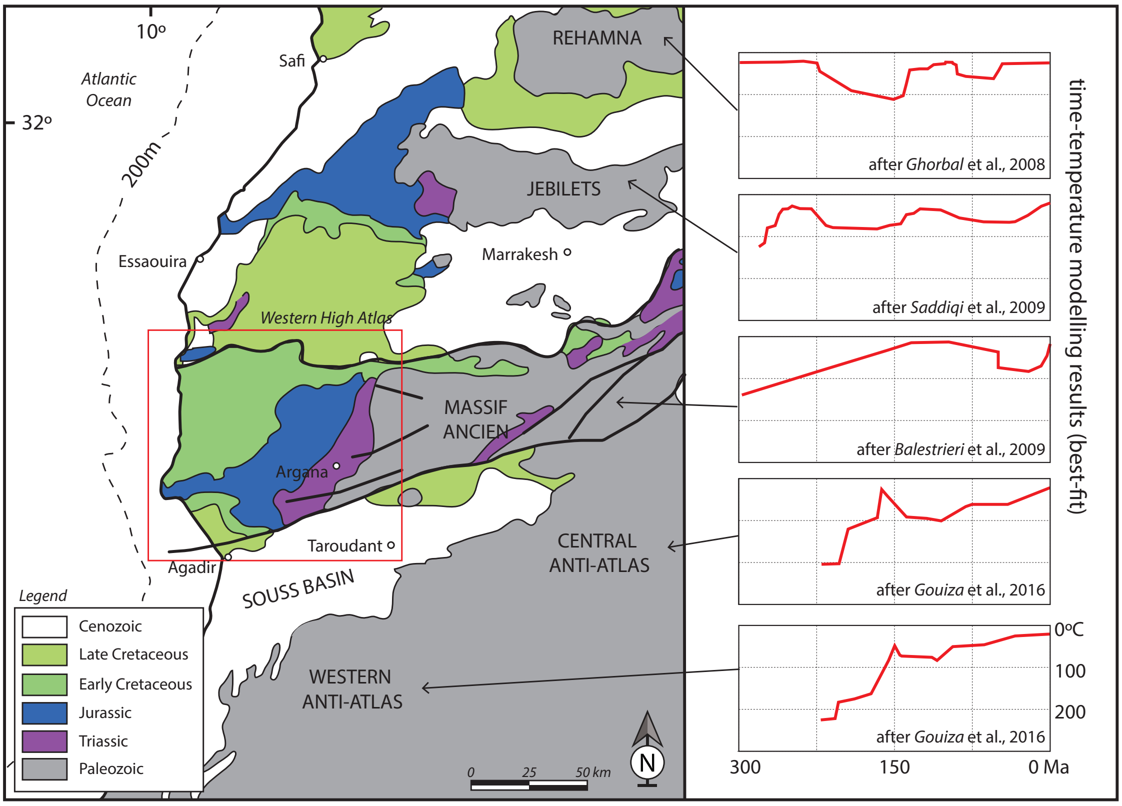

Figure 5: *Vertical movements of different geological domains in the Atlas system (with permission of Rémi Charton (NARG).*

In the Middle-Late Jurassic to Early Cretaceous the entire Atlas region was exhumed [3], [11], [17], [19], which in turn lead to an important period of erosion causing unroofing and exhumation of Paleozoic basement rocks. Initiation of exhumation is diachronus starting at 170 to 145 Ma in the north and 150 to 135 Ma in the south [17]. Subsidence curves from back-stripping geological modeling show subsidence in the Essaouira basin from the Early Jurassic to late Early Cretaceous [14]. Detrital deposits correspond to the Upper Jurassic and part of the Lower Cretaceous, belonging to the post-Atlas rifting period. These movements are only documented by westward tilted pre- and syn-rift successions, which cannot only explained by post-rift thermal subsidence [5]. Subsidence curves from the wells in the WHA, calculated without compaction, show strong subsidence during the Triassic and a period of less subsidence in Jurassic times (fig. 6) [5]. Well TMR-1 (location in fig. 2), however, shows stronger subsidence from the Dogger onwards compared to wells further in the north. Therefore, Middle Jurassic tectonic pulses [34], [40] and even a Middle Jurassic to Early Cretaceous E-W shortening are speculated [5].

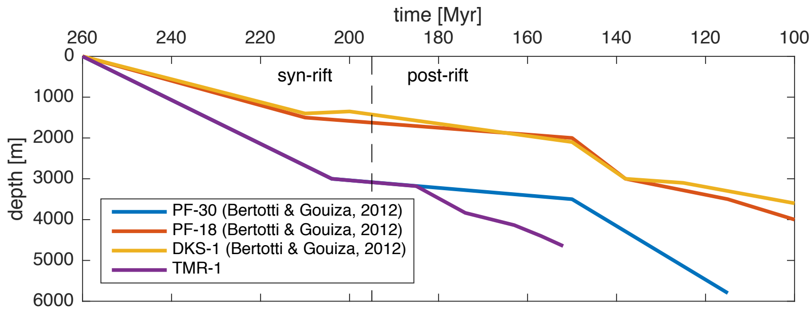

Figure 6: *Subsidence curves for four wells in the WHA (loc. in fig. 2, after Bertotti & Gouiza, 2012).*

Possible compression or shortening can cause folding or salt mobilisation. The folds that are objective of this study are therefore investigated in terms of possibly tectonic forces, especially because the WHA links the vertical movements in the hinterland and the subsidence in the offshore basin. Further, possible exhumation of basement rocks led to erosion and sediment transportation from the mountains towards the offshore. Thus, offshore fan deposits can be linked to exhumation periods in the hinterland with the WHA controlling the sediment transportation pathways and sediment basins.

3 Data Selection & Preparation

The aim of constructing a 3D structural model of two anticlines in the WHA is to understand thickness variations and structural styles in order to characterise possible fold-evolution theories. Google Earth Pro™ (GE) was used as a horizon mapping tool to provide information of x, y and z position of a geologic marker and is based on a DEM. The application of DEM is gaining momentum in modeling topography of the Earth by the geologists, hydrologists, ecologists, geophysics, soil scientists, climatologists, and the specialists working in mineral and petroleum sectors [33]. Geological maps aim to support and identify the horizon that is mapped. A 3D plane-solver plugin in GE allowed for the measurement of large scale dip and dip azimuths in the entire area (http://www.impacttectonics.org/geoTools/3ppfull.html). These are also used to create geological cross sections. Well data was available mainly at neighbouring basins with only a few in the target area. Seismic data was not available. The general flow chart illustrating the input data and modeling approaches is shown in figure 7.

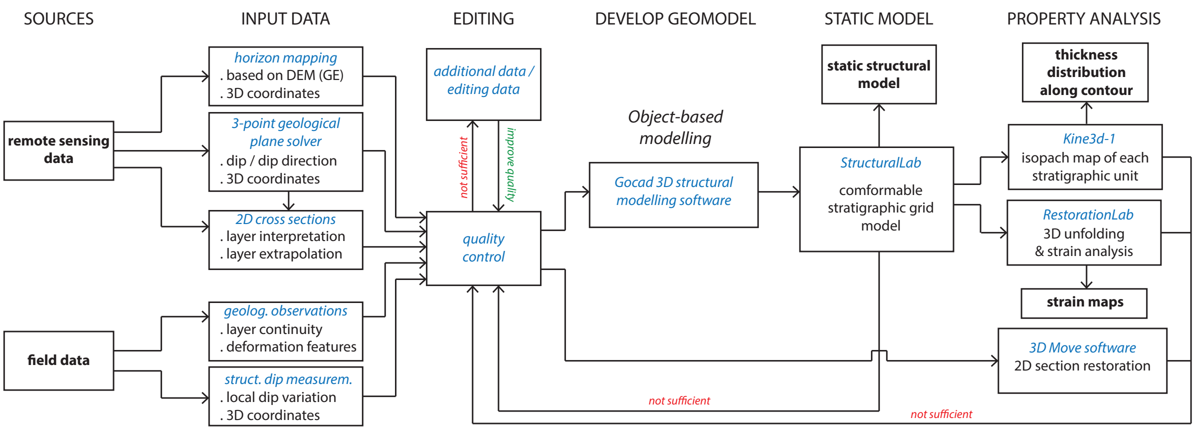

Figure 7: *3D modeling flow chart showing the subsequent steps to produce a static structural model.*

A big challenge of building a 3D model from mainly surface data is the strong anisotropy of information density, meaning that surface data is extremely dense whereas subsurface data is much sparser [9]. Another challenge is the reliability of data depending on the scale of its origin. Field data allows for the study of a geological feature in detail, such as orientation data measured in the field or fault analysis. However, this data are not applicable to a regional model with more large scale trends than local field observations. Thirdly, the variety of data bears a challenge in defining adequate weights to the data points. Perfect data does not exist.

3.1 Geological Mapping & Horizon Interpretation

To built an integrated 3D structural model with sparse data from the region, a new approach of mapping geological horizons at the surface was utilised. Horizon mapping was performed on DEM-coupled satellite images taken at different times to obtain spatial coordinates of geological contacts, identified by colour changes, that are well exposed around the limbs of the anticlines. Google Earth™ elevation data uses Shuttle Radar Topographic Mission (STRM) as its elevation base data [22] and has a spatial resolution of 90m and a vertical error of less than 16m. Since the elevation data is not directly exportable from GE, *GPS visualizer* (http://www.gpsvisualizer.com) allows for quick extraction of bulk elevation data from GE [33]. Mapping the geological contacts along 3D outcrops also provides a better constraint on defining the lateral variations in the geometry of geological surfaces than sparsely distributed field dip measurements [16].

The definition of a stratigraphic marker mapped on remote sensing images is made based on either clear colour changes in the stratigraphy that are easily mappable, as well as from common chronostratigraphic classifications from geological maps. In order to not mix lithostratigraphic and chronostratigraphic data sets, the mapped horizons are based on colour changes (lithology) and are compared for consistency to geological maps (chronostratigraphy). Due to the small scale structures that are observed, there are no strong changes in depositional environment laterally within one fold structure, although there are clear changes between the two folds studied. A list of stratigraphic units translated from the geological map [25] to the model is shown in Table 1.

Table 1: *Stratigraphic markers.*

Geological Map	**Modeled Horizon**	
Top Trias	Top Trias	(T1)
Top Lias sup.-Bajocien	Top Lias	(J1)
Top Bathonian	Top Dogger	(J2)
Top Callovian	Top Callovian	(J3)
Call. to Oxf.	Call. to Oxf.	(J4)
Top Sequanian	Top Oxfordian	(J5)
Top Bathonian	Top Kimmeridgian	(J6)
Top Portlandian	Top Tithonian	(J7)
Top Albian	Top Early Cretaceous	(C1)

3.2 Structural Dip Data

The availability of dip data is necessary to realise a reliable 3D structural model. Due to the large area that the model covers and the regional scale the model represents, dip data was not only obtained from the field. Instead, a *3 point-solver* plugin in Google Earth™ was used. This plugin is based on the concept of knowing the height of a bed of three or more points (not in a straight line) to find the direction of strike and to calculate the dip of the bed [4]. 3D geometrical data is aimed at generating a key horizon that can be used as a template for constructing new horizons [16]. Any geological contact results from the intersection of a geological surface with topography, at which the contact line defines a V-shape as it crosses valleys and ridges [16]. These V-shaped structures are highly present around fold structures, most likely due to the form of erosion based on the fracture pattern that evolves across a fold during its creation and served as ideal locations to measure dip data with the 3D plane-solver. The distance of the three points that need to be picked depends on the size of the structure, such that picking points over distances of more than a few hundred meters was avoided in order to guarantee the reliability of the measurements. However, picking points that are too close would result in an imprecise measurement due to the natural error of the DEM in Google Earth™.

3.3 Geological Cross Sections

Cross sections through the main anticlinal structures better illustrate the geometry of the geological structures and support a more accurate interpolation of the stratigraphic surfaces in *Gocad* and *Move*. They were created using elevation profiles from GE and the horizon mapping, as well as structural dip data. The results provide a better picture of the geometry of the folding. The cross sections were then digitised and georeferenced in *Gocad*. This allows for the simple mapping of the horizons along the cross sections, similar to seismic horizon mapping. These data points can then improve the interpolation of the stratigraphic surfaces.

4 Structural Modeling Approach

4.1 Implicit Stratigraphic Modeling Approach

Gocad offers a plugin to create structural models from sparse geological data using the interpolation function on a tetrahedral mesh. *StructuralLab* honors observation data and faults, such as horizon interpretation curves from remote sensing applications, dip data as a 3D vectorial property and georeferenced 2D geological cross sections (*Gocad* Userguide). These data sets are loaded as separate data according to the conforming sequence which it belongs to. Implicit or level set methods consider geological interfaces as equipotential surfaces of a 3D scalar field [9]. To create such scalar fields from field and subsurface data, two main modeling approaches have been described: (1) Dual kriging and radial basis function interpolation and (2) computation by discrete optimisation on some pre-defined volumetric mesh [9]. The advantage of implicit modeling over explicit modeling is that model updating is simpler with explicit surfaces [9]. The meshing tool in the *Gocad-2009.2* version is a commercial finite element mesher, allowing for the adaption of the mesh resolution to the desired level of detail.

4.1.1 Creating Conformable Stratigraphic Surfaces

To create 3D structural model of the Amsittene and Imouzzer anticlines, all three main sources of data (3D horizon interpretation, structural dip, 2D cross sections) have been loaded to the software (fig. 8) and the *StructuralLab* tool by *Gocad* was used to create comformable stratigraphic surfaces. To obtain sufficient results, at least the top and base, or two stratigraphic units are necessary to interpolate a stratigraphic surface or layer. The interpretation then reconstructs a stratigraphic volume (solid) based on the input data of each stratigraphic horizon. These horizons can then be extracted from the solid.Therefore, the modeling result of one layer is strongly dependent on the surrounding layer. It is important to note that layers can not cross each other in one interpolation.

The outcrop quality of the Amsittene anticline is very good, meaning that all stratigraphic contacts are clearly visible by color changes. A detailed geological map of the area is available from the Geological Ministry of Morocco [25]. The structure suggests that all horizons are comformable and no major faults are disturbing the continuity. Smaller faults were not considered in the model in case they were below the resolution of the DEM used for the mapping. Five geological cross sections enabled a detailed view of the structural geometry of the fold. Combined with dip measurements in between the cross sections and the mapped horizons, a set of nine comformable layers was created.

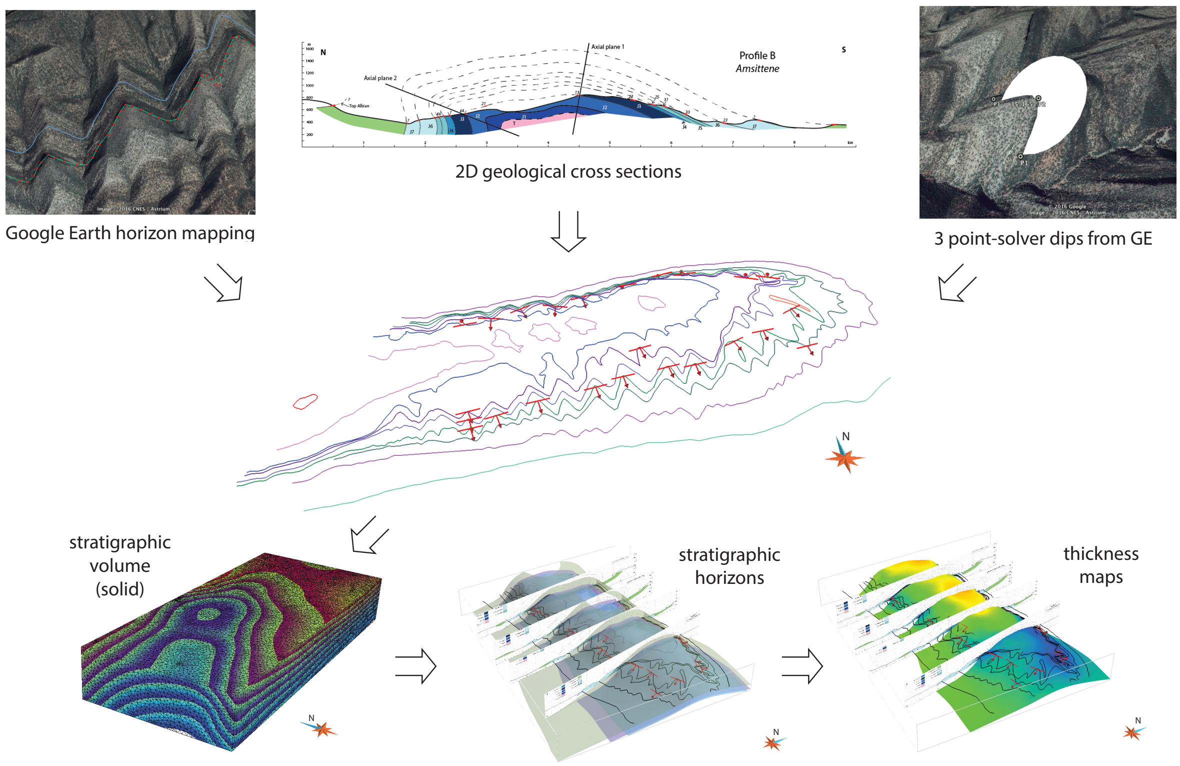

Figure 8: *Data Integration and surface modeling in the Gocad 3D structural modeling environment.*

In the study case of the Imouzzer anticline, two packages of stratigraphic units were modeled separately (iteratively). The reason for that is the otherwise unrealistic results of surfaces using all data traces in the implicit modeling. Therefore, the top of the Lias and the assumed salt surfaces close to the Lower Liassic (solid 1) were modeled independent from the the Dogger and younger layers (solid 2). Implicit modeling techniques allowed for the manipulation of surfaces such that no surfaces crosses another, although extracted from two different solids (or stratigraphic volumes) [9].

4.1.2 Creating Isopach Maps

To create thickness maps in *Gocad*, the *kine3d-1* tool was used as it is able to compute the true thicknesses between two horizons. It constructs a set of normal vectors across a reference surface and measures the distance along that vector towards the above lying layer (fig. 9). Assessing the quality of the results of thickness maps, it is obvious that the most reliable and possibly only reliable results are thicknesses along the contour lines of two horizons. Away from the mapped horizon, the interpretation of *Gocad* becomes independent of any hard data. Therefore, thicknesses in the core and the outer rims of the model are possibly not valid. However, the thicknesses along the contour lines give solid values for thicknesses around the anticline. To better illustrate these results, the surfaces and contour lines were exported and processed in *Matlab* to show thickness along the contour lines.

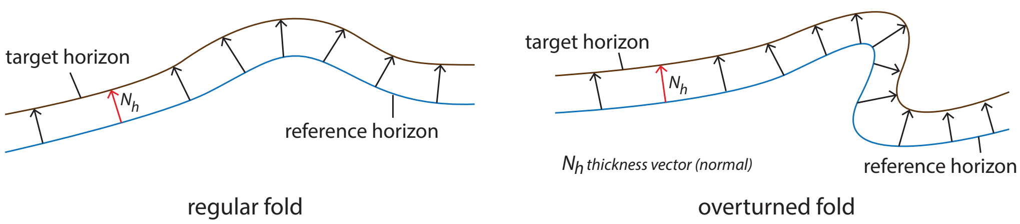

Figure 9: *Kine3d-1 thickness vector calculation in Gocad.*

4.2 2D Flexural Slip Unfolding

Structural restoration is a geometry and geomechanically-based method, allowing for the investigation of the evolution of salt dome structures and strain patterns from folding through geological time [15] or to reduce structural uncertainties by testing the model consistency, quantifying shortening/extension and deformation, and validating interpretations [12]. It can provide geometric information which aids in the understanding of timing of active and non-active salt diapirism. Two methods of unfolding are commonly proposed and used by geomodelers: (1) flexural slip, where shear occurs preferentially along the inter-bed weak layer (shale, silt) and surface of the horizon and thickness are preserved; (2) The simple shear deformation mode with a good approximation of the deformation of granular materials and therefore of the deformation of the poorly consolidated sediments of the extensive areas [31]. Since most rocks in the Jurassic and Cretaceous sequence in the WHA are carbonatic limestones and mudstones and thickness preservation was aimed for in this study, the flexural slip unfolding has been chosen to be as a feasible method.

The *Move* structural modeling software package was used due to its simple and quick 2D restoration workflow, without the requirement of a complex modeling approach, to understand the tectonic evolution of a sequence of geological horizons. The flexural slip unfolding algorithm used in *Move* works by rotating the limbs of a fold to a horizontal datum or an assumed regional surface. Layer parallel shear is then applied to the rotated fold limbs in order to remove the effects of the flexural slip component of folding (fig. 11). A pin line is placed along the orientation at which no slip occurs, namely the fold axis. There are different techniques to determine the position and orientation of the pin line (fig. 10). One way is to geometrically obtain the tangent of a horizon at its inflection point along the limbs and then to find the position and orientation by taking half of the angle where the tangents cross. Another possibility is to determine the orientation of the axial plane in a stereonet by plotting pole points of the fold limbs to determine the dipping angle of the axial plane. However, this second method does not provide the position of the axial along the cross section. *Move* relies on three principles for flexural slip unfolding: (1) line length is preserved in the unfolding direction, (2) area of the fold is maintained, (3) true bed thickness is constant. This also results in an area conservation [31].

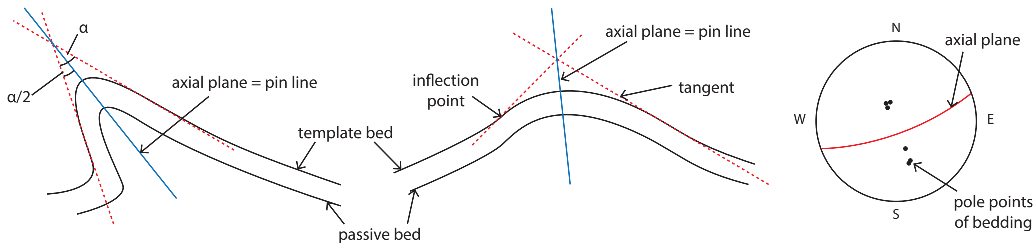

Figure 10: *Different techniques to determine the position and angle of a pin line (no slip).*

Unfolding is performed using the cross sections created earlier in the process since these are the only hard data points from the anticline. The horizons are traced along the four cross sections perpendicular to the strike. It is important to note that the horizon traces are purely interpretative and thicknesses are not reliable in the fold core. The unfolding results still represent a good estimation of the overall tectonic signal in a section perpendicular to the fold strike. An additional cross sections along the fold axis might give insights into changes in tectonic signal in another direction. This is done by creating a surface from lines along cross sections only using the Delaunay Triangulation method. This ensures that there are no numerical errors in the interpolation of the surface behaviour in between the cross sections. A new cross section is then created cutting the surfaces parallel to the fold axis, which is also unfolded. This method provides a pseudo-3D view on the anticlinal structure at certain tectonic stages.

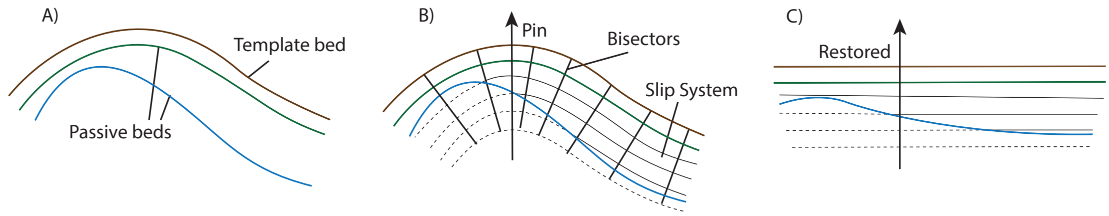

Figure 11: *3D Flexural Slip Unfolding in Move using a pin to define non-slip areas along the hinge line.*

4.3 3D Unfolding & Strain Analysis

Strain distributions provide information about the location and orientation of deformation or fractures [12]. To obtain strain eigenvalues and tensors from a 3D structural model, restoration steps are performed in order to reconstruct sedimentary successions to its original depositional state by removing the effects of tectonic forces. Durand and Caumon (2009) suggest a 3D modeling approach in *Gocad* to efficiently model strain in complex structural domains [12]. Their paper discusses that tectonic deformation can be simplified to plane strain or simple shear with difficulty, and hence should be addressed with a true volumetric approach. The method or Implicit stratigraphic modeling in a 3D stratigraphic volume (or solid), computed from efficiently from scattered data, has been described in the previous chapters. These volumes can now be restored and used to model strain.

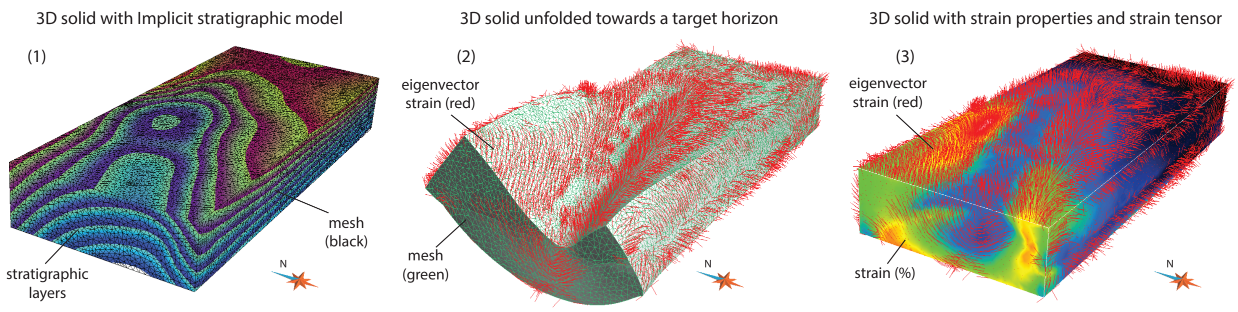

Figure 12: *3D unfolding and strain analysis procedure in Gocad.*

Gocads RestorationLab plugin restores 3D stratigraphic volumes (fig. 12(1)) to a pre-deformation state of reference level (the uppermost horizon) within the volume (fig. 12(2)). One boundary is fixed along a certain axes which will not move during the unfolding. The retrodeformation, computed from the deformations between the current configuration and the restored one, is then displayed on the volume (fig. 12(3)).

4.4 Accuracy, Uncertainties & Model Validation

Elevation data collected by remote sensing methods, such as elevation profiles of geological contacts mapped in Google Earth™, provide the basis for the outcome of this project. Recent studies have proven the reliability and accuracy of the Google Earth™ DEM data, and suggested its use being reasonable to support most application areas including research [22], [33]. The resolution of DEM's used in Google Earth™ is given with a resolution of 90m and a vertical error less than 16m [38]. Especially in mountainous areas, the quality of Google Earth™ data is adequate and comparable to other sources, such as ASTER DEM's, providing a spatial resolution of 15 to 90m [33], [38]. However, studies concluded that Google Earth™ DEM is not perfect in representing steep slopes, and also, the correlation analysis is indicates a linear relationship in the elevation data [33]. Compared to freely available SRTM datasets, the Google Earth™ DEM, which is also based on SRTM data, shows significantly better resolution and accuracy [33]. This may be related to the continuous refinement of elevation data in Google Earth™ through successive addition of high resolution data from other sources as they become available for different areas [44]. Still, when other elevation data sources are available, such as LiDAR with a horizontal resolution of 1 to 2m and vertical resolution of 20 to 30cm [33], the results could be substantially improved.

Errors and uncertainties occur in two different domains: (1) the numerical domain including the digital data used, as well errors caused in the computational modeling approach and (2) the user domain, in which errors are created manually. Numerical uncertainties are the resolution of the DEM used in the picking of horizons, which also affects the quality of the dip measurements acquired with the 3-point solver plugin in Google Earth™. Comparing dipping angles and orientations measured in Google Earth™ to those measured in the field, field measurements show no large difference (± 10%). However, in some carbonate outcrops in the Amsittene anticline, field measurements gave much steeper dipping angles (60°) than the Google Earth™ measurements (25°). In this case the larger scale Google Earth™ dips have still been used to represent the layer orientation, since the carbonate rocks seemed to have been post-tectonically locally tilted by gravitational down-hill forces. Another source for uncertainties is given by the surface modeling approach in *Gocad*. Results are only sufficient in areas close to the data points, i.e. horizon contours, dip measurements or cross sections. For example, thicknesses calculated in between these hard data points are not recommended to be used as proper results due to the interpolation method giving a strong variance in thickness and unreasonable absolute values. Errors caused by the user include mainly the horizon picking on Google Earth™ and the dip measurements, which were often difficult to obtain in areas with high vegetation or when the geological horizons have similar colours or are less pronounced in the morphology. Further, interpretation of layer continuity in cross sections is often driven by subjective decision-making, but is also limited due to the sparse data available. This has a large impact on the 2D unfolding scenarios and tectonic signals interpreted.

5 Results

5.1 Amsittene Anticline

The Amsittene anticline is located in the northern part of the Western High Atlas basin, having a E-W trending strike-orientation extending over a length of around 30km with a width of 6km. Towards the west the fold is covered by Quarternary sediments until it disappears into the offshore where its continuation is not clear. The middle and eastern part reveal all Jurassic formations until the fold dies out in the east. Four cross sections perpendicular to the strike were made in order to identify the geometry of the fold and to determine possible processes explaining the structural evolution, such as deformation features caused by mobile salt deformation or indicators of a compressional genesis. A geological map of the Amsittene anticline is shown in figure 13.

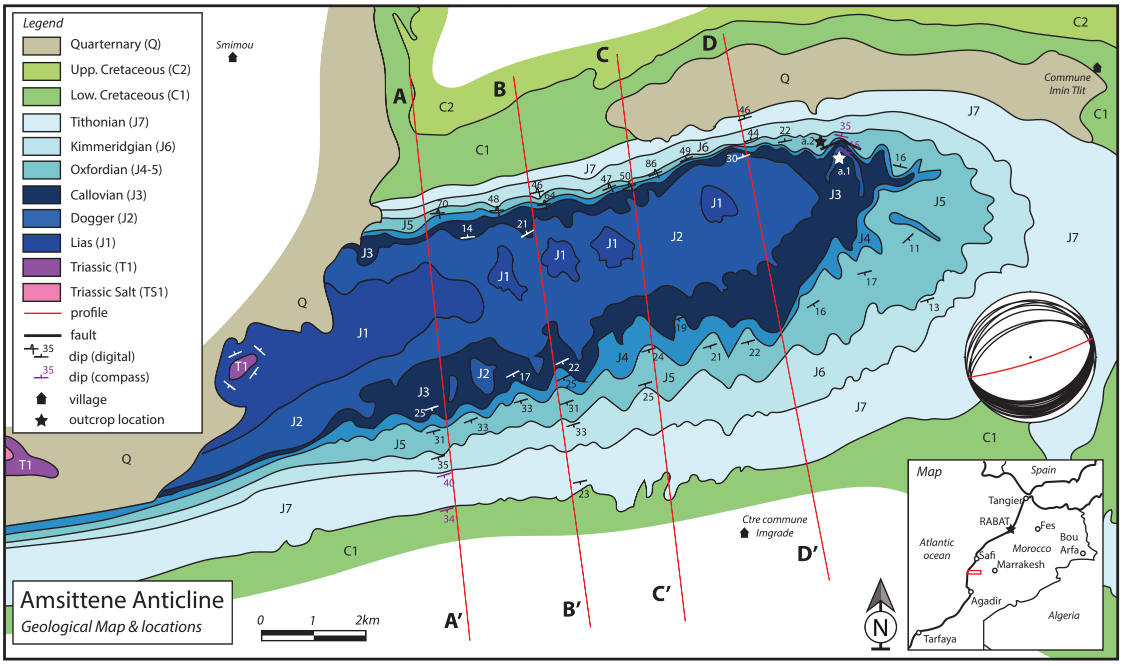

Figure 13: *Geological map of the Amsittene anticline illustrating the locations of outcrop studies, structural data and position of the geological profiles.*

Dip measurements using the 3-point plane solver in Google Earth™ allows for the determination of the geometry not only along cross section in the field, but around the entire structure. Therefore, 38 dips were measured from mainly clear geological horizons along V-shaped erosional valleys at the fold flanks. The results show that the northern flank of the fold is overturned from 70 to up to 40° dipping SSE in the Oxfordian, and regular bedding in the east with dips of 20° to 30° NNW (fig. 13). The southern flank is not overturned, but showing relatively constant dips of 25° to 30° SSE (fig 13.). Stereonet analysis yields an average axial plane dipping 85° slightly towards WSW. Salt is cropping out in two salt mines in the Western part of the fold. Dip measurements around the smaller salt prove the dipping of layers away from the salt in a circular shape and an intrusive contact [6], suggesting active diapirism and local extrusion of salt.

5.1.1 The Amsittene 3D Structural Model

The structural model of the Amsittene anticline reveals an elongated fold structure with 20 to 30° dipping bedding planes in the southern limbs and a more complex, partly overturned section in the northern part. The structure can be characterised as an elongated subvertical fold gently plunging to the East. The fold disappears towards WNW, whereas it is not possible to reconstruct the continuity of the fold towards the

East. The anticline has two different axial planes, one that is more or less vertical in the southern part of the fold and one that is inclined towards the North, making the whole structure an asymmetrical, in some parts steeply inclined, fold.

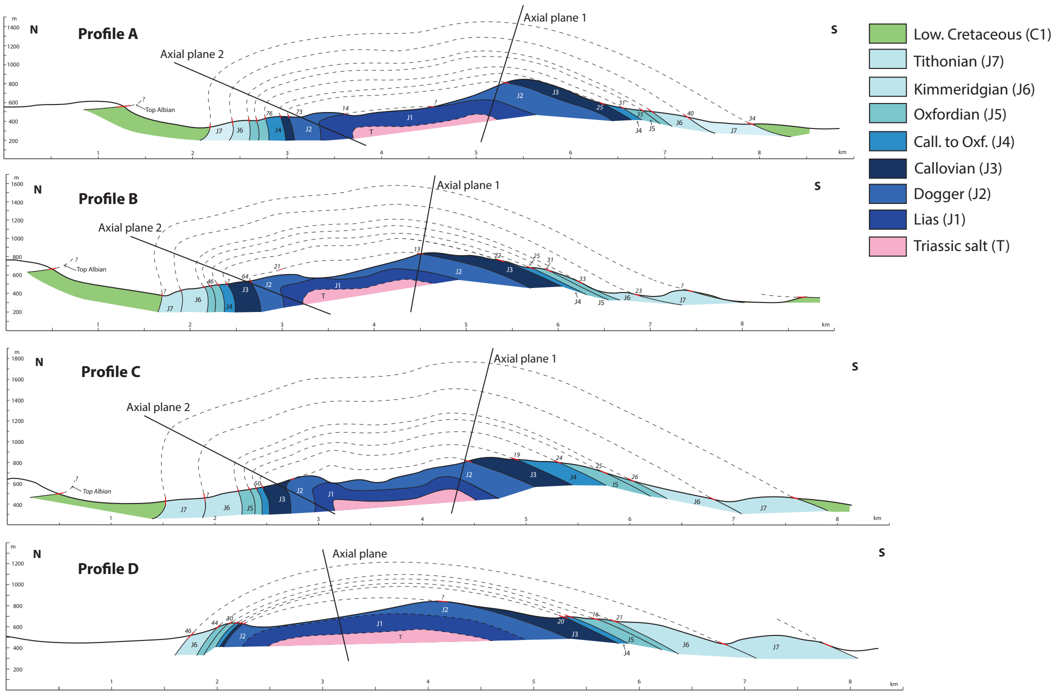

Figure 14: *Cross sections through the Amsittene anticline used in the modeling process.*

Figure 15 (left) shows the 3D structural model of the Amsittene anticline with modeled horizons from the Triassic to the Tithonian (not all shown). From the implicit stratigraphic modeling process it is possible to also extract the top of the salt (fig. 15, right). Clearly, the salt is not homogeneously distributed along strike. In fact, it forms a dome structure in the eastern part. In the center part the salt is more shallow and has some local elevated areas, for example where the salt crops out in a salt mine.

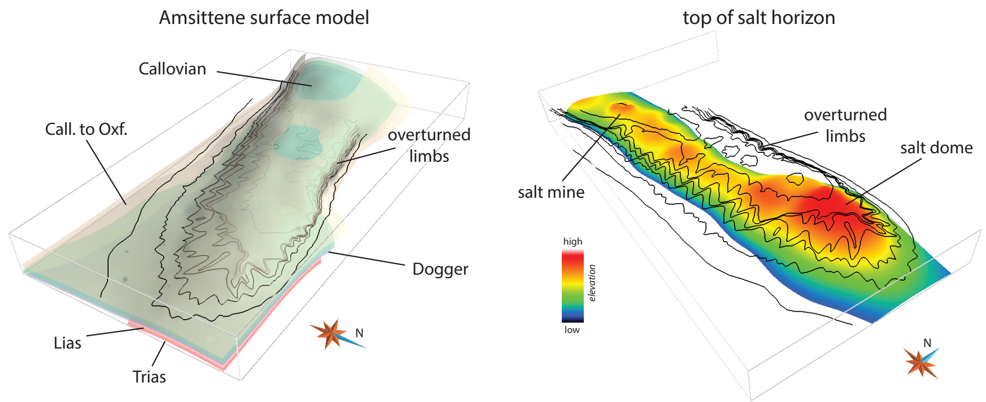

Figure 15: *modeled surfaces (left) top salt elevation (right) in the Amsittene anticline.*

5.1.2 Thickness Variations

Thickness variations suggest the presence of depocenters in the Jurassic. Depocenters showing a different orientation than the current geometry of a fold suggest a different orientation of an anticline in the past or possible salt activity throughout the Jurassic.

The results of the 3D structural model reveal an along-strike change in thickness of Jurassic sediments. Figure 16 shows the thickness variations, comprising the Lias, Dogger, Callovian, Oxfordian, Kimmeridgian and Tithonian, along a clockwise profile from the northwestern to the southwestern end of the fold. The profile unveils a thickness decrease from the overturned northern flank towards the east with a substantial decrease in thickness at the point where the fold limbs change into NNW dipping beds. It is noteworthy that all formations follow the same trend. In the southern limbs, towards the west, the thickness of all formations increase progressively, never reaching the same thickness as in the northern limbs. Generally thickness is never constant over more than 5km.

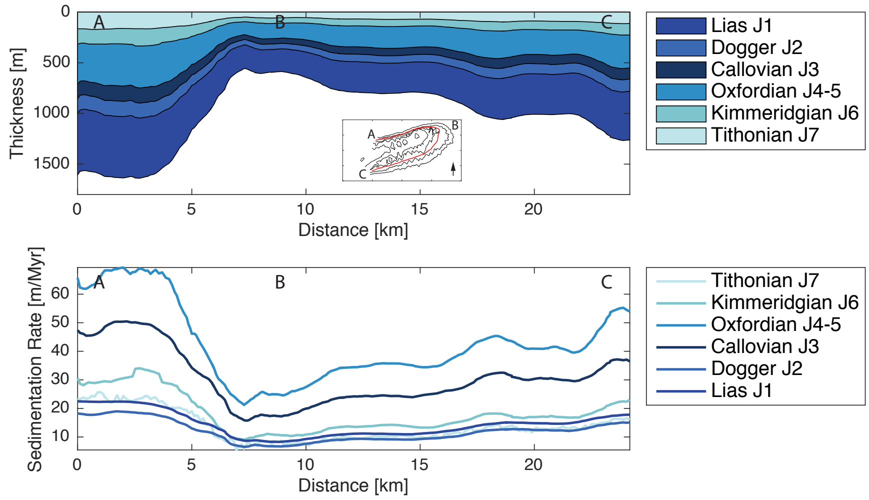

Figure 16: *Thickness variations and sedimentation rates for Jurassic sequences in the Amsittene anticline..*

The thickness distribution along the contour lines of the respective geological contacts are shown in figure 17. Maximum thicknesses are present in the overturned layers, although numerical thickness calculations in those parts are often difficult. Thickness at the eastern side (at around location a.1 on map) yields around 40 to 50m in the Callovian and 140m and 80m for the Oxfordian and Kimmeridgian, respectively. Towards the southern limbs sediments get thicker yielding 140 to 200m for the Callovian, which corresponds to an increase in thickness of about 70 to 75%.

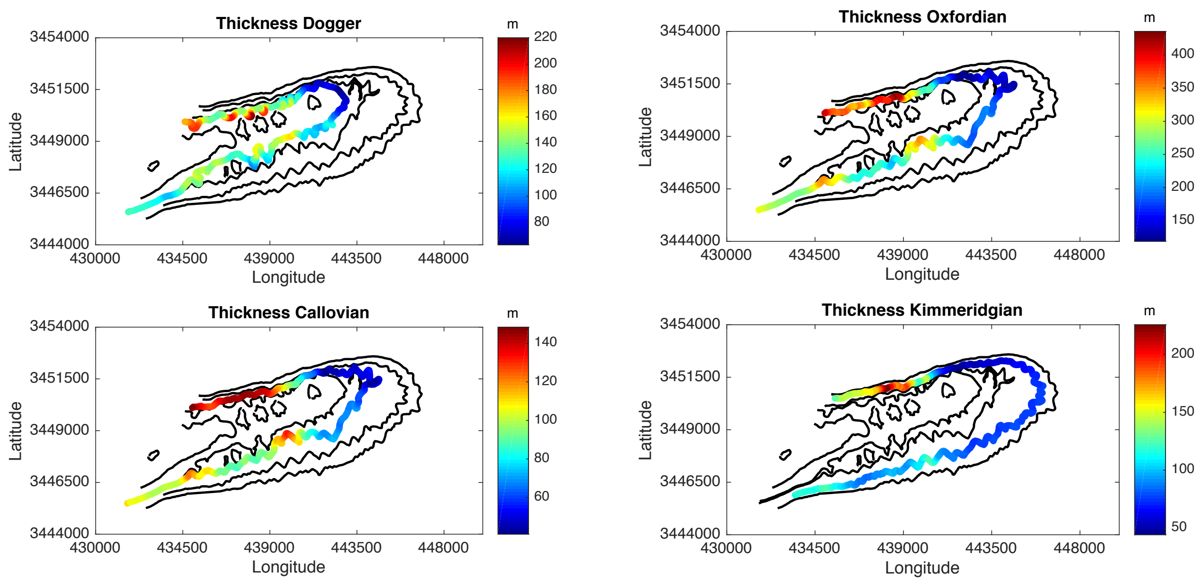

Figure 17: *Thickness changes along contour lines of Jurassic sequences in the Amsittene anticline.*

The Oxfordian strongly increases from around 140m to more than 300m and only the Kimmeridgian is slightly increasing in thickness (from min. 50m to max. 100m). The resolution of the model suggests a precision of around 20m and therefore lies below the thinnest sedimentary beds modeled in the Amsittene anticline. The thickness distribution suggests a depocenter in the northern part of the anticline and an area of less deposition in the eastern part throughout the entire Jurassic.

5.1.3 2D Unfolding & Restoration

2D flexural slip restoration was performed on four cross sections perpendicular to the strike of the fold (A, B, C and D) and one cross section parallel to strike, close to the hinge line (E). The pin line had to be placed through the axial plane of the strongest deformed areas of the fold, although more than one axial plane was obtained from most cross sections. Profile A, B and C cross the overturned northern limbs of the fold. Profile D has no overturned limbs.

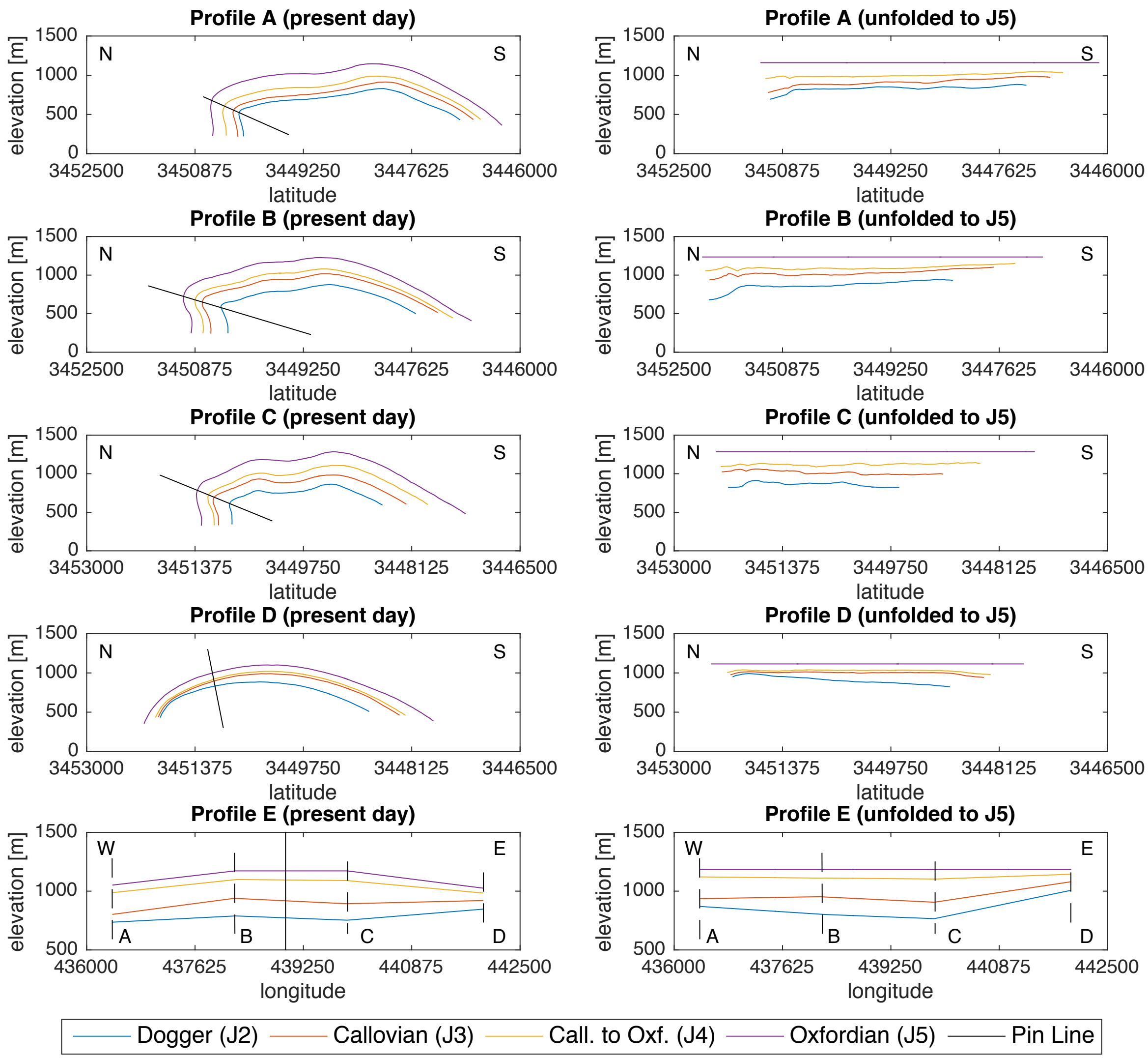

Figure 18: *2D flexural slip unfolding in the Amsittene anticline, restored to the Oxfordian (J5).*

The results show the structural geometry of the fold at the time of the Oxfordian. The Alpine shortening is therefore supposed to be removed. The oldest considered and clearly mappable horizon is the Dogger formation. The results are illustrated in figure 18. When unfolded, profile A and B show a clear trend of northward thickenning and all horizons follow the same trend. Towards profile C, the thickenning trend changes to a northerwards thinning, which becomes even more clear in profile D. The Dogger and Callovian show a stronger thinning trend than younger formations. Depositional depocenters must have migrated to the south. The strike-parallel profile clearly shows a thinning towards the east (D) and therefore a sediment depocenter towards the centre of the anticline (B and C). From the Dogger to Oxfordian, the eastern part must have been exhumed before the Alpine shortening (D), because the flattened profile shows upward dipping of Early Jurassic layers towards the east. A similar, but less clear trend can be observed in the west (A).

Table 2: *Amount of shortening in the Amsittene anticline.*

Section	A	B	C	D	E
Shortening	13.2 %	12.7 %	13.8 %	7.5 %	0.14 %

The amount of shortening in all cross section is listed in Table 2. Tectonic shortening in N-S direction is largest in section A, B and C with around 13 %. Towards the west, in section D, tectonic shortening reduces to 7.5 %. In the E-W direction the tectonic shortening is only 0.14%. However, this value might be imprecise since not the entire fold length could be modeled in the hinge parallel profile.

5.1.4 3D Unfolding & Strain Analysis

3D unfolding was performed on a selection of formations, similar to the 2D flexural slip unfolding. All horizons have been unfolded or flattened to show the cumulative strain over time. In the Lias and Dogger, strain is largest in the overturned northern limbs of the fold, at which most deformational features and faults are most pronounced. In the southern limbs, deformation mainly occurs in the southwestern part, soon diminishing towards the east, where the fold is disappearing. The Callovian and Call. to Oxf. show the same pattern although strain is a little less in the centre of the fold. All horizons have an increased strain in the area where salt is outcropping in a salt mine in the western centre and all horizons show an asymmetrical strain distribution.

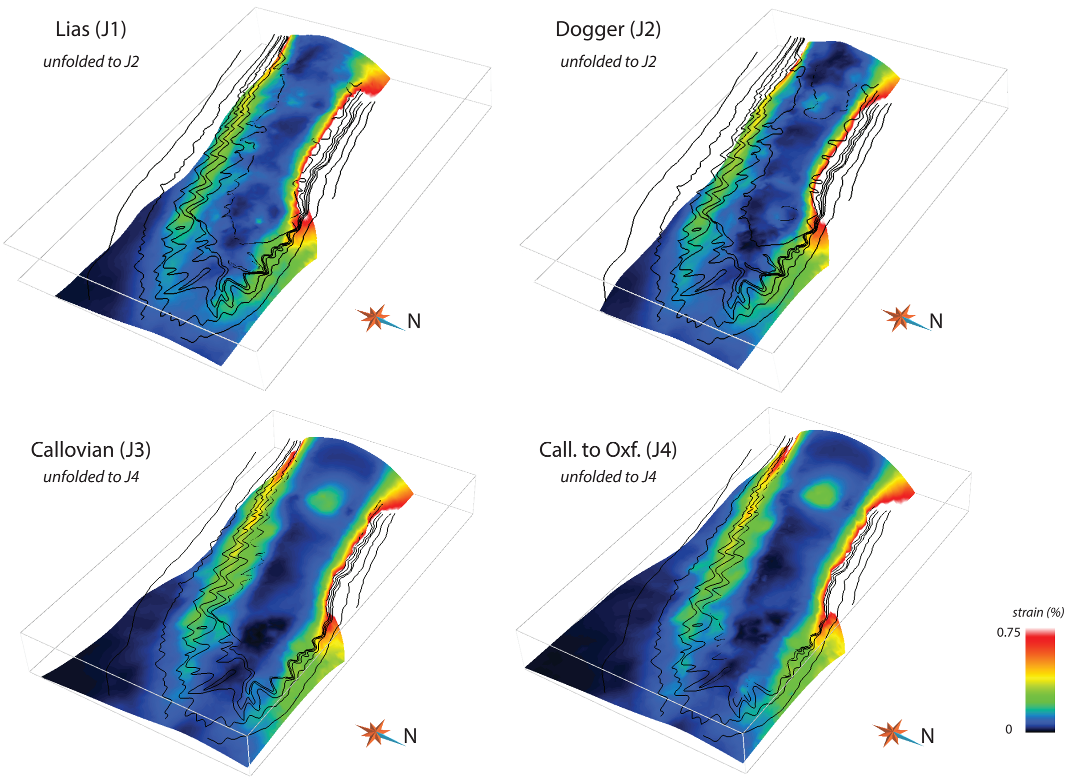

Figure 19: *Strain in the Lower to Middle Jurassic in the Amsittene anticline.*

5.1.5 Field Study

On the northeastern side of the anticline at location a.1, the Dogger to Kimmeridgian are exposed (fig. 20, C). A cliff of almost 15m of carbonate rocks, most likely Dogger to Callovian rocks, shows discontinuous layers forming onlap structures. Onlap occurs towards the south, i.e. the center of the anticline. These onlaps result in a thickening of more than 5m over a distance of about 50m towards the north (fig. 20, C). This results in a change in dip from 25° in the upper section to 20° and 15° in the lower section.

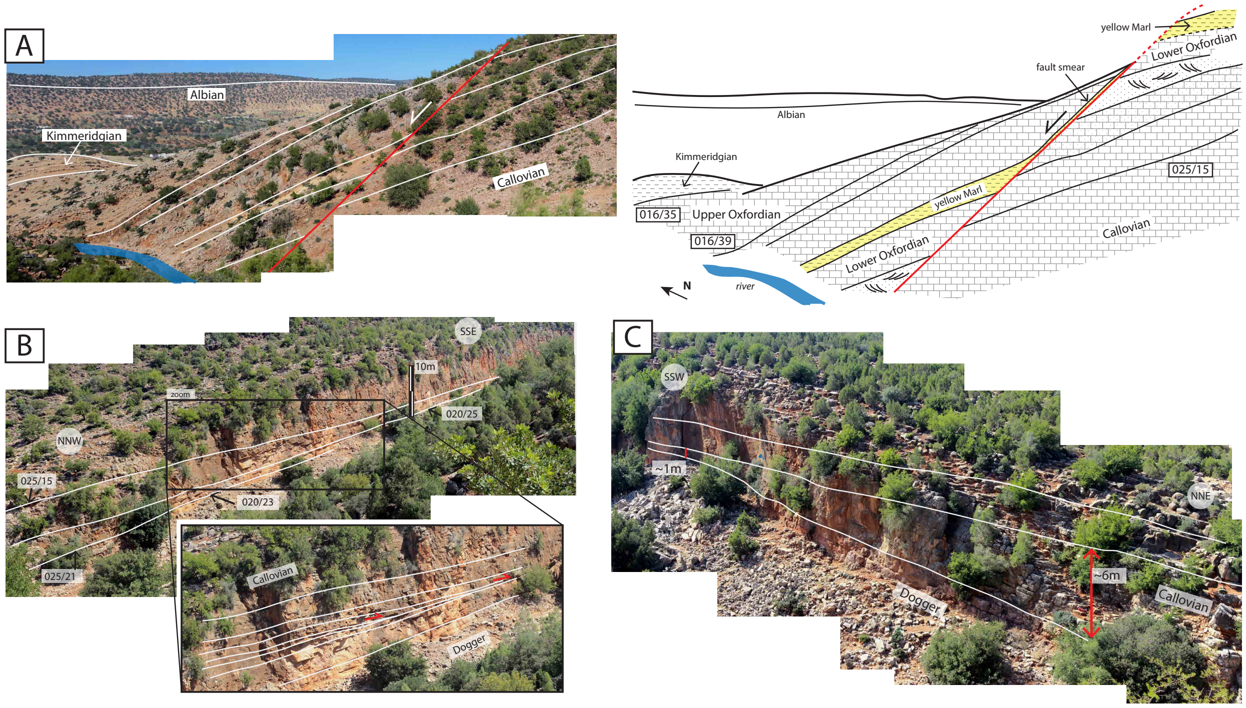

Figure 20: *Normal faulting (A) and syn-sedimentary onlap structures in the Dogger to Callovian (B,C).*

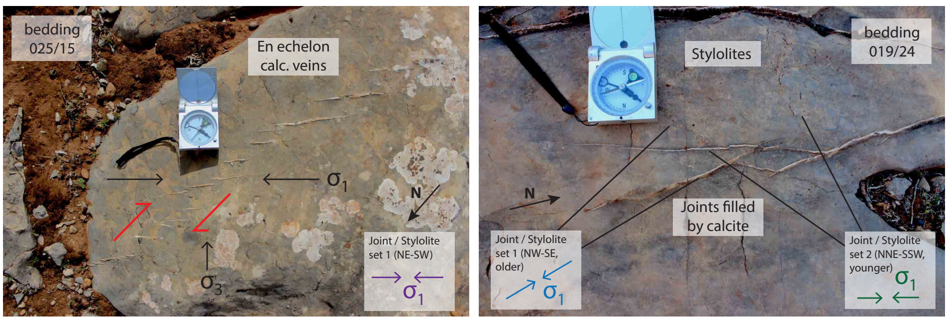

Figure 21: *Left: Calcite filled en echelon veins suggestion a NW-SE compression in Callovian rocks. Right: Two different sets of joints and stylolites indicating NW-SE and NNE-SSW compression.*

Figure 20A shows a large normal fault cutting the Oxfordian with a displacement of around 50m (location a.2). The axial plane is dipping 60° to the North. The fault zone is characterised by a cataclasic fault zone and marl smeared out on the fault. The yellow marl, which is also visible on satellite images, is the key feature to determine the style of displacement and to measure the displacement itself. Indications for a compressional stress regime with regional shortening, are given by en echelon structures, joints, and stylolites, which are not parallel or perpendicular to bedding. They indicate a shortening direction of roughly NE-SW, although joints and stylolites in figure 21 indicate two different stress directions, one NW-SE and another one NNE-SSW. The latter seemed to have occurred later in time, since the joints connect pre-existing fractures or veins and do not cross them. Still, these features show that the anticline has previously been involved in two different tectonic shortening events, later than the Callovian.

The obtained field observations only provide a very local view on the geological features pointing towards a solution or possible interpretation of the fold structure. The normal fault present in the north-eastern part of the anticline, for instance, was not considered in the model since it is too small to play a bigger role in geometry or thickness distribution. However, field observation could prove the relative thicknesses at certain positions and give insights on small geological features that are not observable using remote sensing methods, but which clearly lead the geologic discussion towards the driving factors of folding.

5.2 Imouzzer Anticline

The Immouzer anticline is a roughly 10km long and 4km wide Jurassic fold structure in the Agadir-Haha basin in the Western High Atlas (location fig. 2) and exposes Jurassic formations from the Lias to Kimmeridgian. Figure 22 shows a geological map of the Immouzer anticline including structural data and the locations of the outcrop studies. Stereonet analysis suggested that the fold has an axial plane oriented NE-SW, being slightly tilted towards the SW.

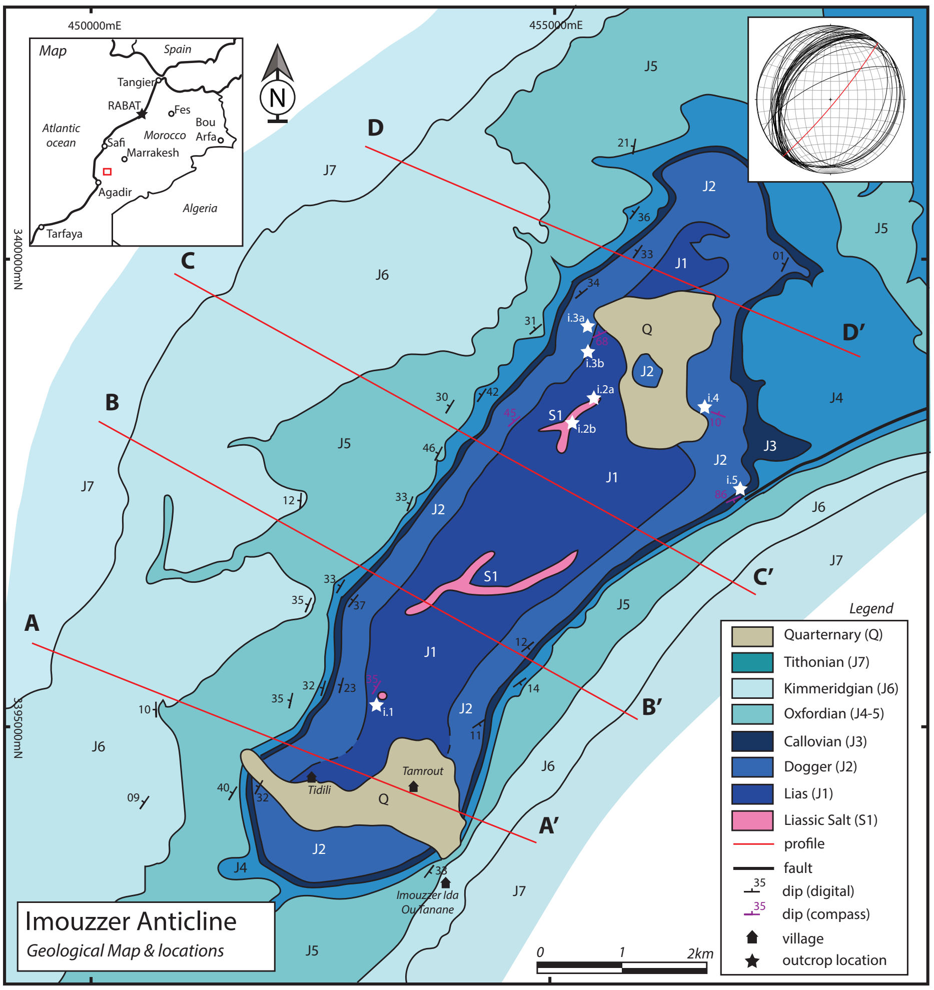

Figure 22: *Geological map of the Imouzzer anticline illustrating the locations of outcrop studies, structural data and position of the geological profiles.*

5.2.1 The Imouzzer 3D Structural Model

The stratigraphic contacts were mapped on Google Earth™ along colour changes from one lithological formation to another, but no reliable geological map was available. The available maps mostly disagree on the position of Middle Jurassic horizons that do not fit the satellite images. Recent sedimentary erosion and deposition covers some regions in the lower and upper part of the anticline. The Dogger is an ideal marker due to its protruding red colour in between the yellowish Lias below and the massive cliffs of the Callovian above. However, the contact between the Lias and Dogger in the most northern and southern rims of the anticline is hardly visible. Four geological cross sections were made using the exact location of the contacts and the dip angles taken from Google Earth and the field (fig. 23).

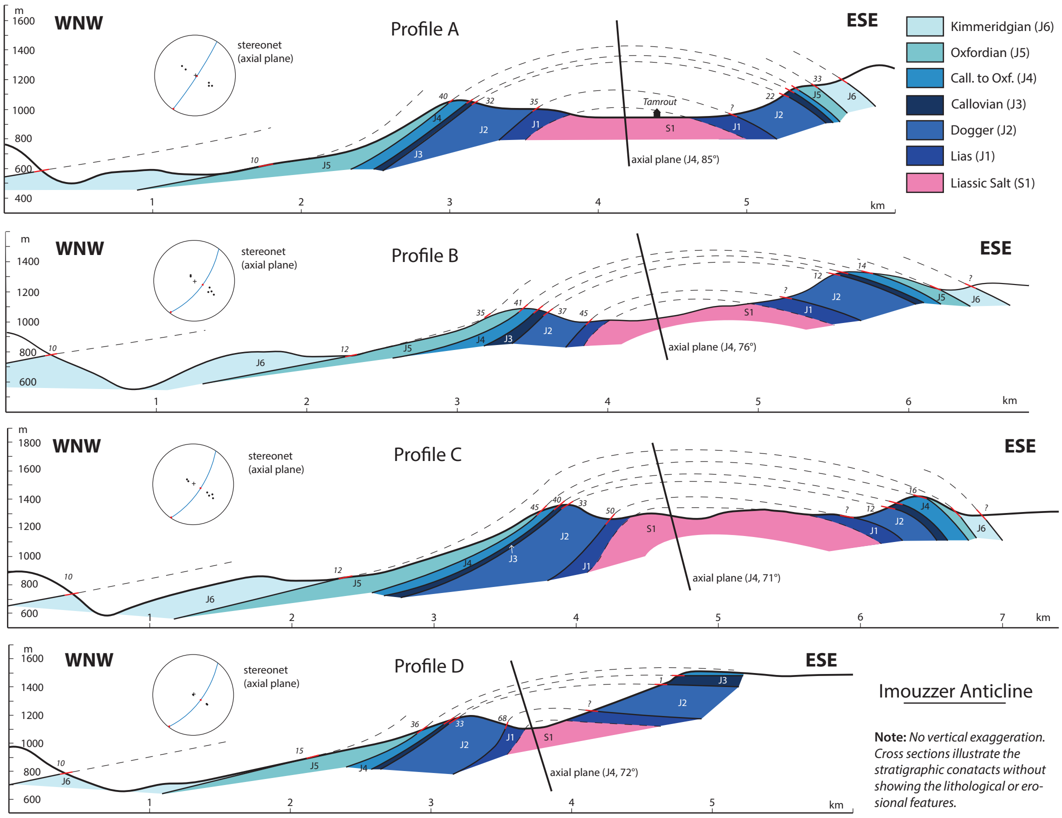

Figure 23: *The four cross sections illustrating the structural style of the Imouzzer anticline.*

The structural model of the Imouzzer anticline comprises horizons from the Lias to Kimmeridgian (fig. 24 not all shown). The fold can be interpreted as a gently inclined fold with a hinge plane dipping towards the SE. All horizons are continuous and no major faults disturb the stratigraphic succession. Large scale dip variations from the field were added to the data obtained by remote sensing methods. Looking at the top of the salt within the Lias, the model suggests a dome structure in the centre of the anticline, but it is less pronounced towards the NE and SW, where the fold disappears.

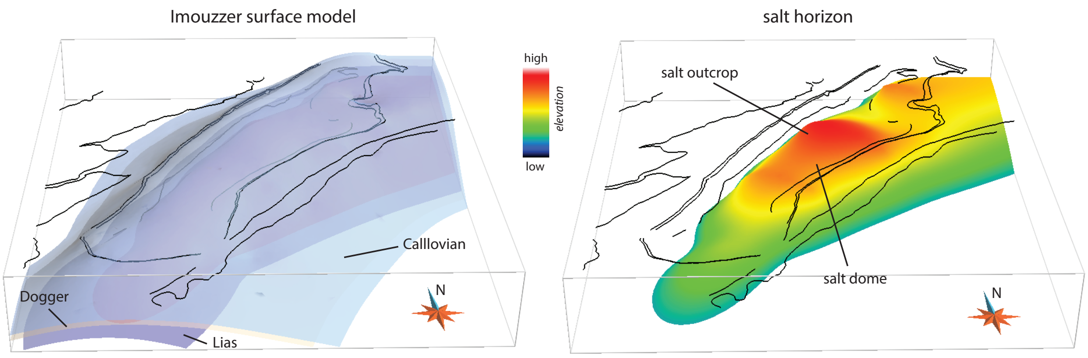

Figure 24: *modeled stratigraphic horizons (left) and top of salt surface (right) in the Imouzzer anticline.*

5.2.2 Thickness Variations

Similar to the Amsittene anticline, thickness maps were created in the Imouzzer anticline to detect possible changes in sediment distribution. The calculated thicknesses are only valid along the contour lines obtained from remote sensing mapping. Away from these points, the model becomes interpretative and stochastic, and are therefore not used. Further, only results from the Dogger and Callovian are illustrated, due to the fact that the Oxfordian and Kimmeridgian outcrop data points lie too far apart to provide reliable data of true thicknesses. Still, these two formations used here seem to be crucial to understand the tectonic evolution of the anticline, since field observations suggested strong differences in deformational features and thickness distribution.

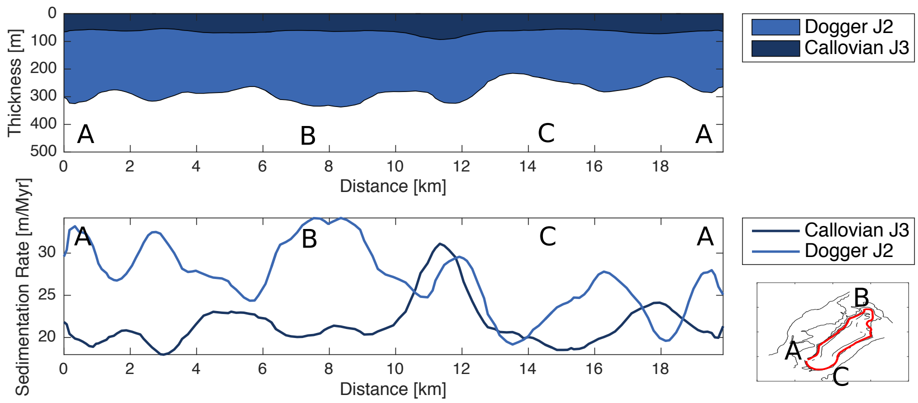

Figure 25: *Thickness profile and sedimentation rates of Jurassic sediments in the Imouzzer anticline*

The Dogger shows strong thickness variations along the entire profile (fig. 25). Thicknesses in the Dogger ranging from around 150m to almost 330m. There is no decisive pattern in the thickness distributions of the Dogger, meaning that thickness varies locally at different locations along the anticline (fig. 26). However, strong thickness variations occur near places where salt deformational features have been found, which will be shown in the following chapters.

The Callovian is relatively constant in thickness throughout the entire profile with thicknesses of around 80m. It is not following the thickness trends of the Dogger, rather, it shows thickening at places where salt was found (location i.3, fig. 22). The strong increase in thickness of the Callovian in the eastern part (thickness of up to 95m) is likely due to a recent geological event. Sedimentation rates, assuming that they were constant within a stage, were higher in the Dogger, compared to the Callovian. Similar to the thickness distribution, they do not follow clear trends or orientations along the anticline.

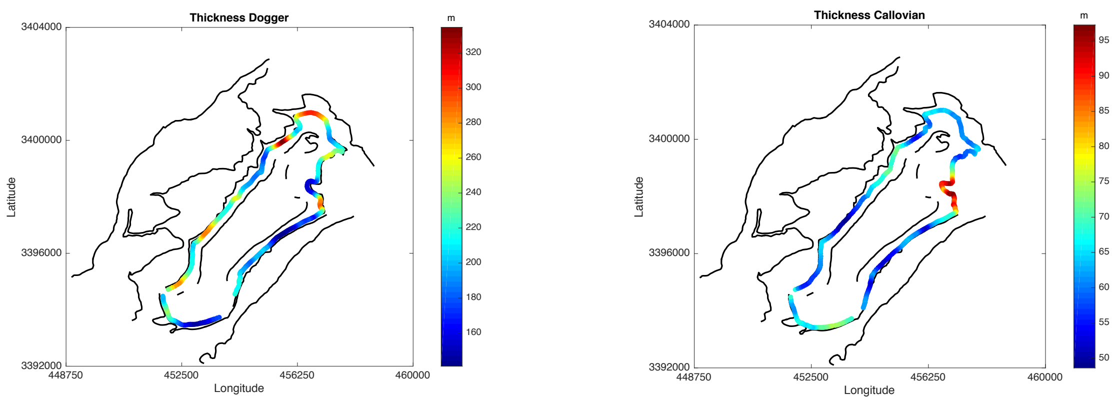

Figure 26: *Thickness changes along contour lines of Jurassic sequences in the Imouzzer anticline.*

5.2.3 2D Flexural Slip Unfolding

For the Imouzzer anticline the orientation of the fold axial plane of each cross section was used as a pin line, since it can be assumed that the present day fold geometry is derived by the Alpine compression, which is supposed to be removed (fig. 27). From the existing cross sections (fig. 23) the surfaces were created similar to the Amsittene anticline. These surfaces were then used to create a new profile along-strike the anticline (Profile E, fig. 27).

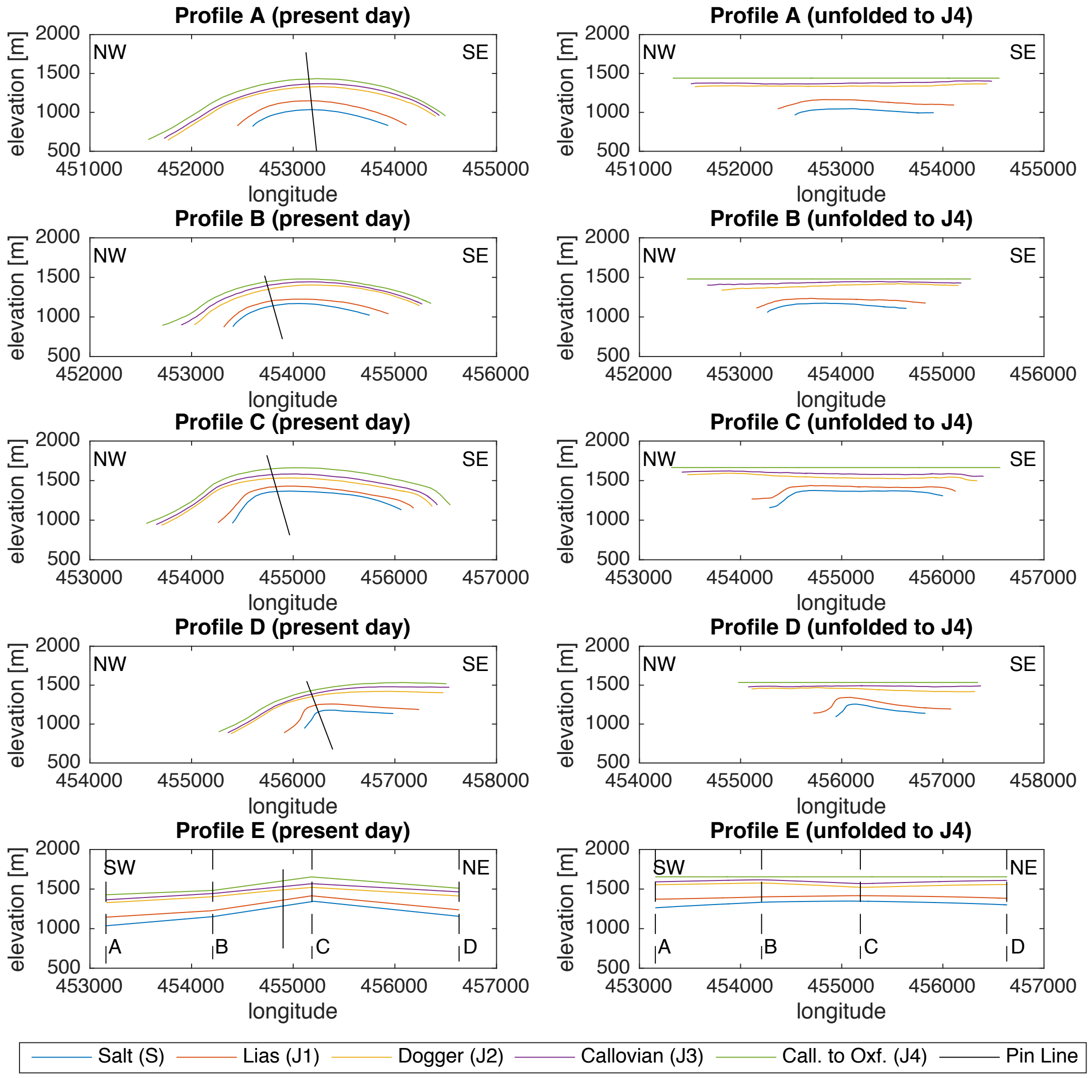

Figure 27: *2D flexural slip unfolding in the Imouzzer anticline, restored to the Mid Oxfordian (J4).*

The results show the structural geometry of horizons during the Mid Oxfordian (J4). There is a clear difference in the tectonic imprint of the Lias and its salt compared to that of the Dogger and younger formations (fig. 27). Hence, in the Mid Oxfordian, sediments have been deposited horizontally above a pre-existing anticlinal structure in the Lias. There are no clear thickness variations or differences in tectonic imprint along the fold axis. However, it appears that profile C is slightly more exhumed compared to the other sections at present day.

The amount of shortening varies from 9.5 to 5.6% in all cross sections orientated NW-SE (Table 3). There is no trend or directions to which the amount shortening decreases or increases. However, the SW-NE trending cross section E gives a shortening of 0.2%.

Table 3: *Amount of shortening in the Imouzzer anticline.*

Section	A	B	C	D	E
Shortening	9.5 %	5.9 %	8.1 %	5.6 %	0.2 %

5.2.4 3D Unfolding & Strain Analysis

3D unfolding in the Imouzzer anticline illustrates the location of areas with higher strain when horizons are unfolded, i.e. flattened. Each horizon was unfolded or flattened completely to illustrate the cumulative strain of a formation over geological time. Figure 28 depicts the strain in the Early to Middle Jurassic and demonstrates a different strain distribution over time. In the Lias, the strain concentrates in the NW area and covers also central areas of the fold, but almost no strain is observable towards the SW and NE where the fold disappears. At the top of the Dogger towards the Call. to Oxf., the strain is concentrated in the limbs following the strike of the fold. Maximum strain is arranged in an elongated pattern parallel to the strike orientation with larger strain values in the western flank compared to the strain in the eastern flank.

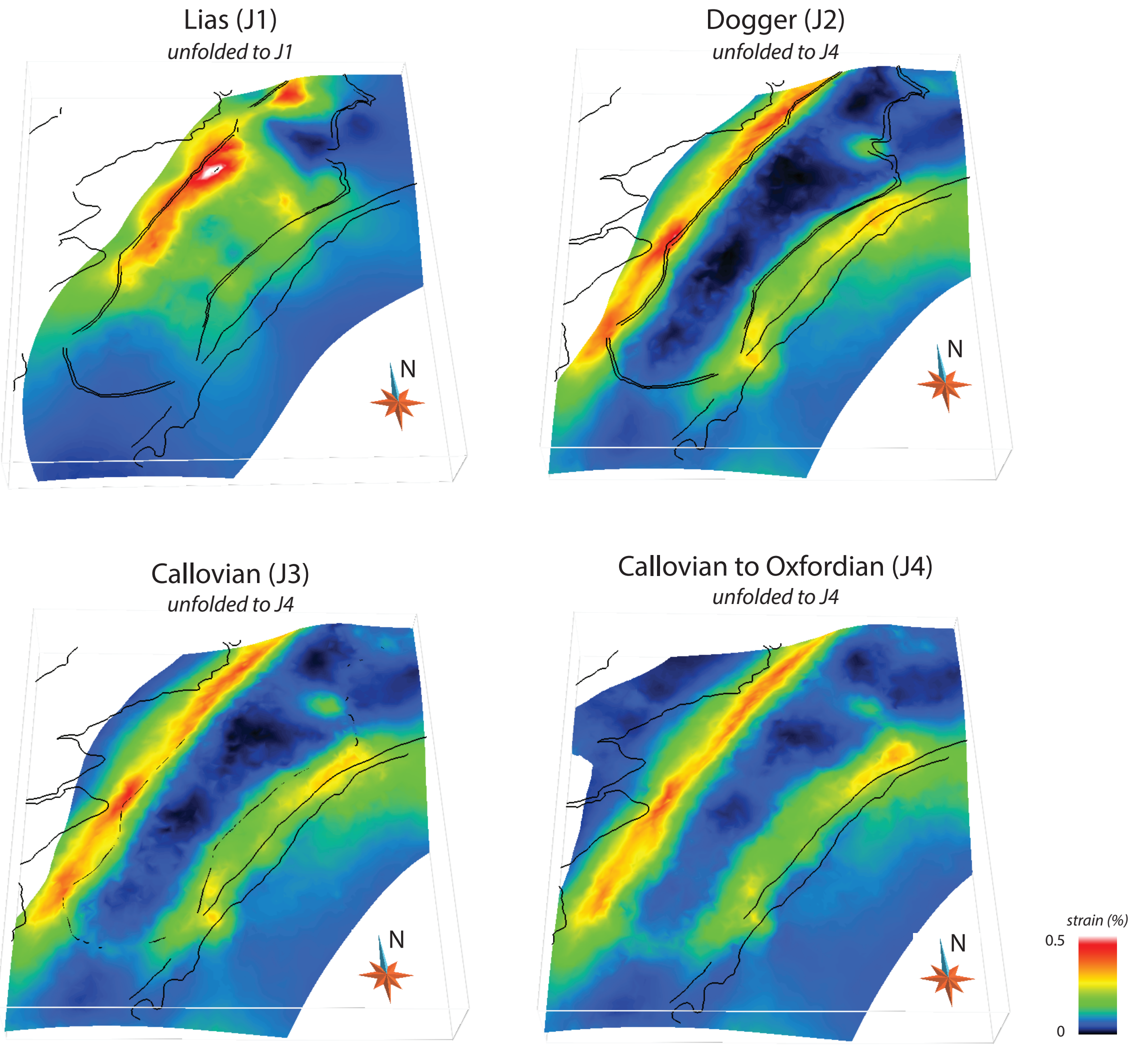

Figure 28: *Strain distribution in the Lias, Dogger, Callovian and Call. to Oxf. (Imouzzer anticline).*

5.2.5 Field Study

The core of the anticline comprises poorly exposed Liassic limestones that are mostly covered by recent erosional sediments. Liassic rocks are generally outcropping in riverbeds, whereas in the south and north-east they are generally not exposed at the surface. North of the village Tidili the Lias is dipping NW showing no large deformation features. In the Northern part (location i.3), Liassic sediments dip 68° NNW, forming a conformable contact to the Dogger. On the opposite side of the anticline, layers are dipping towards SE. Thick layers of salt (gypsum) are interbedded in carbonatic layers of the Lias (location i.2). Salt layers are dipping NE following the morphology of the fold core (fig. 29 A).

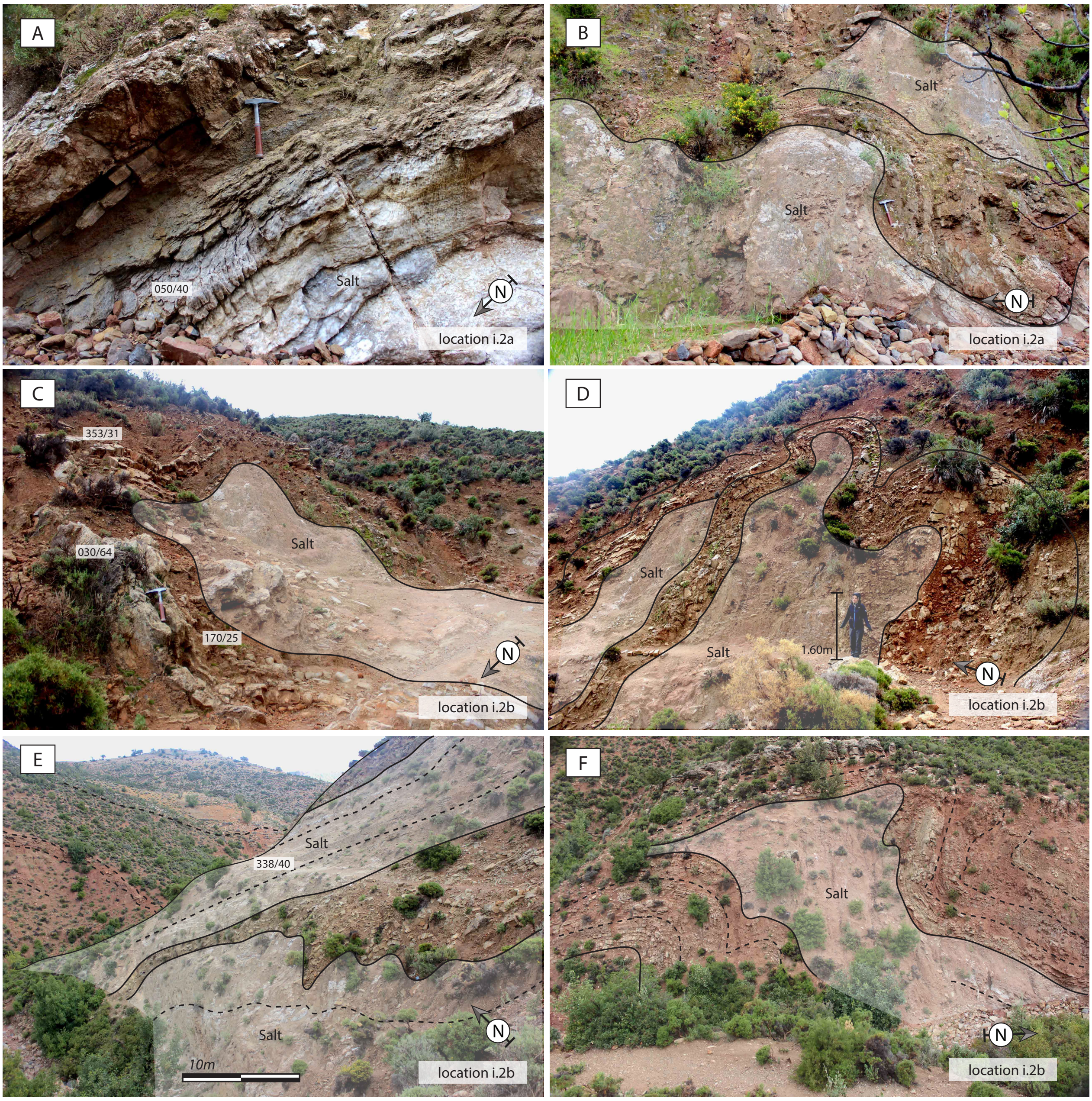

Figure 29: *More than 50m thick Liassic salt outcrops showing strong salt deformation features.*

Deformation of the carbonate layers interbedded in the salt are found all along the the valley, showing multiple folding structures and diapir intrusions (fig. 29 B, C, D, F). The orientation of the bedding is different from the general trend of NW dipping layers at the western flank. The thickness of the salt can be assumed to amount at least 50m, since the base of the salt is not visible.

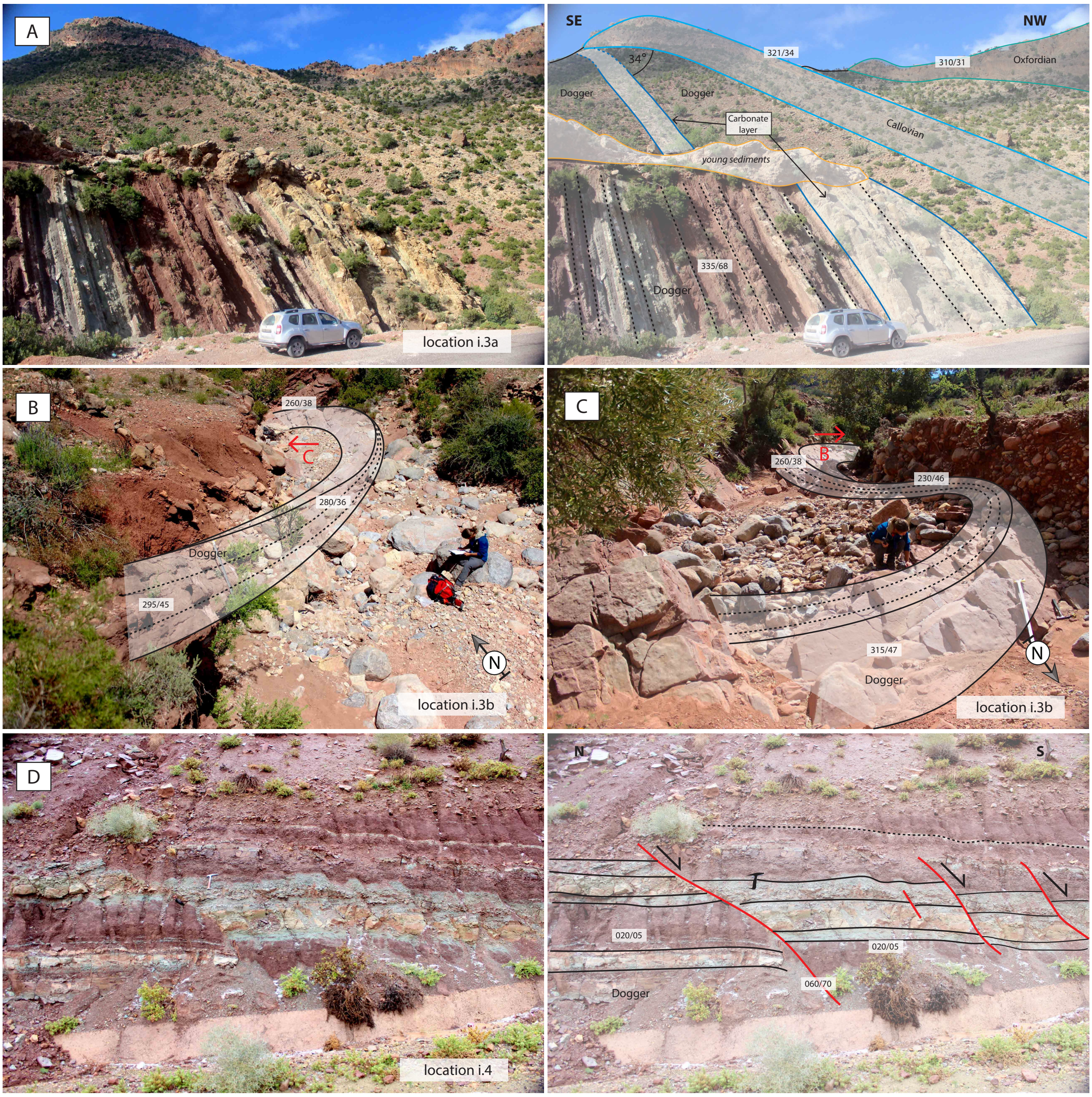

Figure 30: *The Dogger showing an angular unconformity (A), folding (B,C) and normal faulting (D).*

The contact to the yellowish rocks of the Lias to the reddish rocks of the Dogger is comformable. The marly to sandy deposits of the Dogger, with thicknesses of 200 to 250m, are strongly deformed. Folding is observed at the base, whereas towards the top deformation features are of a faulted nature, showing normal faulting and smaller fold structures (fig. 30 B, C). Generally, the NW dipping trend of the layers is continuous along the eastern limb. The small normal fault along the road on the western flank is dipping towards the NW, however, the marly components of the Dogger are too soft to break, meaning that these features are only visible in the smaller interbedded sands or carbonate layers. Changing thickness of those layers from S to N of a normal fault might indicate syn-sedimentary deformation (fig. 30 D).

The transition from the Dogger to Callovian is characterised by a change in depositional environment, resulting in a change from reddish sediments to thick and massive carbonate sequences made up by reefs. The contact from Dogger to Callovian is probably uncomformable (location i.3), showing an angular unconformity (fig. 30 A). Here, the top of the Dogger, with steep dipping layers compared to the Callovian, was eroded and the Callovian was deposited on top. The contact angle between the two is extrapolated to approximately 30°, meaning that the Dogger might have had a structural dip when the Callovian was deposited. The strike orientation of the sediments from the Dogger at that position varies from around 10 to 20° from the fold axis. From a structural point of view, the Callovian is a compact, continuous and widely undeformed sequence compared to the Lias and Dogger below. Folds can be found only at a few locations along the ridges. At location i.5 along the Northeastern flank the Callovian is dipping vertically. The Oxfordian and Kimmeridgian is not present in the erosional core of the anticline, except some Oxfordian reefs near Tidili showing large forsests of carbonate reefs. Towards the NW both layers are shallowing in dip from around 30° to around 10° showing strong deformational features. At the SE side of the fold the layers of the Oxfordian and Kimmeridgian are shallow to horizontal in the middle part of the anticline.

6 Discussion

6.1 Structural Evolution of the Anticlines

6.1.1 Regional Thickness Trends

Structural modeling on two anticlines in the WHA revealed the thickness of Jurassic sediments at these locations. To clarify the salt activity in the region and their influence on these folds it is important to understand the regional thickness changes, especially away from and in between anticlinal structures. A strong increase in thickness in between anticlines would indicate the formation of minibasins due to active salt diapirism forming anticlines.

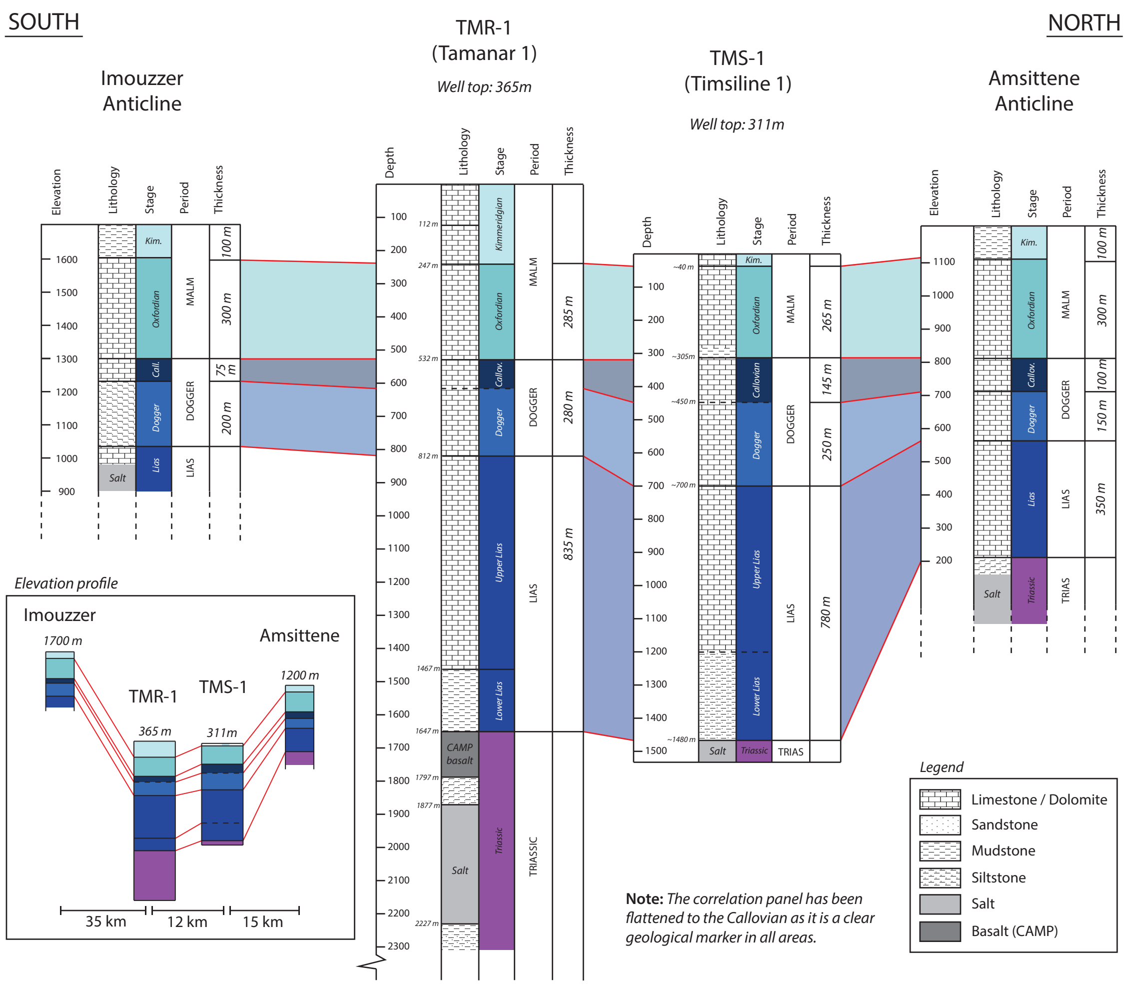

Figure 31: *N-S Correlation panel through basin (loc. in fig. 2, wells with permission of NARG & Onhym).*

Therefore, two wells located in basins in between the two studied anticlines (note that the wells actually represent much smaller anticlines), have been used to create a well section including the outcrop information from the model data (fig. 31). The correlation panel shows no large thickness gradients, indicating that there was no a large salt diapir moving upward, forming minibasins in between the anticlines. Instead, the Dogger, Callovian and Oxfordian are surprisingly constant in thickness. Only the Lias is thickening from the Amsittene anticline towards the south, although information on the Liassic thickness is missing from the Imouzzer. Still, Early to Middle Jurassic sediments are always thinnest in the anticlines.

6.1.2 Timing and Structural Style of Fold Growth

Large Triassic salt basins and offshore seismic surveys in the Agadir-Essaouira basin demonstrate large salt diapirism, forming large-scale anticlines [21], [43]. The Jbel Amsittene and Imouzzer anticlines were studied in order to characterise depositional trends, deformation patterns and thickness changes to better understand the timing of fold growth in the WHA. The alpine N-S compressional phase can be assumed to have significantly overprinted these structures in the Western High Atlas, making it difficult to extract the compression or salt-induced growth in the Mesozoic [29].

Amsittene anticline This anticline is an asymmetric anticline with overturned limbs in the north and salt domes in the fold core. Evaporites are found in Triassic sediments in the Western part of the anticline and a larger salt dome in the East. Field studies revealed syn-sedimentary onlap structures, normal faulting and asymmetric thinning of sediments, proposing active salt diapirism during the Dogger, Callovian and likely the rest of the Jurassic to Early Cretaceous. Alpine shortening certainly overprinted the fold structure from the Late Cretaceous onward. Overturned limbs are likely a result of the Alpine shortening of pre-existing diapiric anticlines [8]. Joints, en echelon structures and stylolites in Callovian rocks indicate two different shortening directions. The NNE-SSW compressional features can likely be linked to the Alpine shortening. The NW-SE, however, is either a result of an earlier local rotation of the compressional axes within the Alpine orogeny, or pinpoints towards a much earlier compressional event, maybe in the Middle or Later Jurassic, which led to the mobilisation of the salt and an early stage of fold growth. Results from the 2D restoration modeling indicate a different tectonic signal in the Eastern part of the Amsittene anticline within the Dogger, where syn-sedimentary features have been documented, but not in the central part along the fold axes. Modeling of the top of the salt suggests one single salt dome in the East and another smaller dome in the Western part, cropping out in a salt mine. Possible faults or thrusts were debated before and indications are given in seismic lines [6], [21]. However, the resolution and quality of the seismics, as well as the absence of a large fault at the surface dismiss the possibility of a thrust-fold reaching the surface. Still, a fault in deeper formations is possible and the importance of faults and fault blocks on salt activity in the area was already discussed [34], [42].

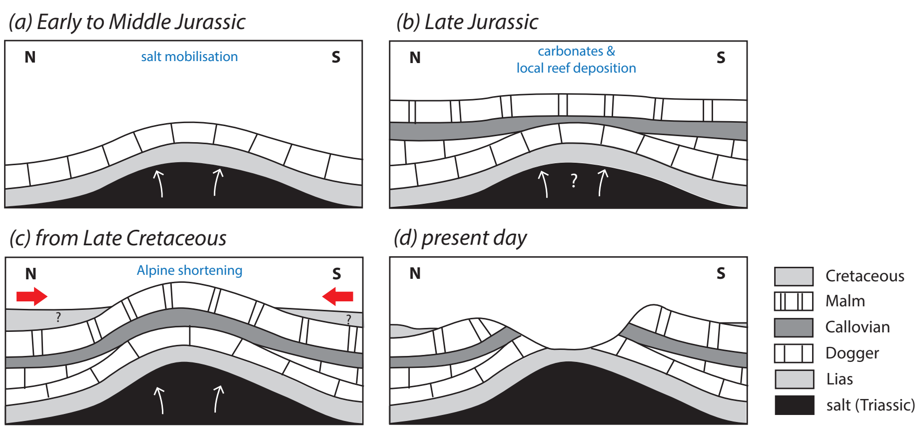

Figure 32: *Conceptual model for the Amsittene anticline with active diaprism in the Jurassic.*

Immouzer anticline The Imouzzer anticline in the southwestern part of the Haha basin is a salt cored, elongated anticlinal structure exposing folded Liassic to Oxfordian sediments. Evaporites with thicknesses of more than 50m and beautiful but chaotic salt deformation structures prove that the salt was active during the Lias and Dogger. This is further proven by the observed deformation features in the soft Dogger sediments, whereas the overlying Callovian does not show these features. The thickness distribution derived from the 3D model reveals strong fluxes in the Dogger, but constant thicknesses in the Callovian, suggesting that the salt was inactive during the Callovian. Further, Oxfordian carbonate reef foresets in the Tidili section document the aggradational growth of a carbonate platform possibly caused by the subsequent fold growth. 2D flexural-slip unfolding also confirms a different tectonic signal in the Lias and Dogger, compared to the younger sediments when removing the alpine tectonic shortening. Figure 33 illustrates a conceptual model for the evolution of the Imouzzer anticline from the Lower Jurassic to Upper Cretaceous. Upward moving, Liassic salt formed an anticlinal structure during the Lias and Dogger, which strongly deformed the two units and possibly led to erosion at the top of the Dogger. Salt movements must have ceased during the Callovian, possibly forming an angular unconformity. Middle Jurassic unconformities and time gaps were already documented in the WHA and were explained by a phase of tectonic uplift [40]. Folds developed on the sea-floor and led to the formation of large carbonate reefs and reef foresets (i.e. in the Tidili section), especially around the anticlines. The location and characteristics of those reefs, as well as the influence of Jurassic folding, could not be tested with the methods of this study, but are part of a sedimentological study currently carried out by the NARG team. The Alpine compression, orientated roughly N-S, caused further steepening of the fold, deforming the Middle to Upper Jurassic stratigraphy that also caused erosion and the top which formed the morphology at present day.

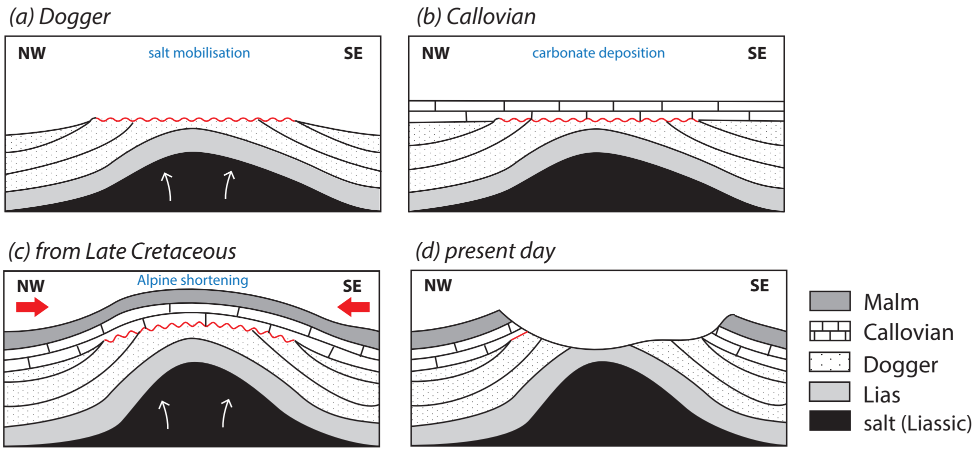

Figure 33: *Conceptual model of the Imouzzer anticline with active diapirism in the Early to Middle Jurassic.*

Active salt diapirism generally causes a thickenning trend away from the anticline or in between diapirs. This is difficult to prove from the modeling results. Therefore, a N-S correlation panel from the Imouzzer to the Amsittene anticline and two wells in the syncline demonstrate thickness variations in the Jurassic away from anticlines. Thickness is hardly changing in the Middle to Upper Jurassic. Only the Lias shows a southward thickenning away from the Amsittene anticline, changing from about 300m to almost 800m. Unfortunately, the base of the Lias is not exposed in the Imouzzer anticline. This, however, suggests that larger movements of Triassic salts occurred during the Lias, leading to the deposition of smaller minibasins. Liassic salts, such as those present in the Imouzzer anticline, do not contribute to the formation of minibasins or similar. These intercalated salt layers within carbonates are not comparable to the thick Triassic salts, although they appear to be thick. Therefore, it seems that only Triassic salts are able to cause larger anticlinal structures in the basin. Liassic salt is likely to only cause local salt mobilisation at a much smaller scale, but is still able to create topographic changes in the Early to Middle Jurassic.

Comparing the hypothesis made here to other areas a lot of similarities have been found. The timing of salt mobilisation and active or inactive diapirs in the Central High Atlas (CHA) has been well described by Saura *et al.* (2013). They observed onlaps indicating active salt movements in the Lower, upper Lower and Lower to Middle Jurassic [39] (fig. 34). The scale of salt movements in the CHA are much larger than what was observed in the WHA at the example of the Amsittene and Imouzzer anticline. Still, salt cored ridges such as the Tazoult ridge have similar dimensions forming a southward leaning canopy around 2km wide at its crest, similar to the Imouzzer anticline. Additional common features are Middle Jurassic strata (Bathonian to Callovian) sealing salt ridges and thus recording the end of its diapiric activity [39]. Although the salt mechanisms in the offshore Agadir-Essaouira area are certainly different from those onshore, timing of salt cored folds and diapirs are similar to those observed in recent studies by NARG and others, onshore [32] (fig. 34). A study from Bertotti and Gouiza (2012) about the Tidsi anticline in the northern vicinity of the Amsittene anticline, suggested regional shortening to explain structural observations and Middle Jurassic to Early Cretaceous exhumation and syn-sedimentary deformation in the Essaouria-Agadir basin. An unconformity separating Triassic from Portlandian and a significant increase in thickness of the Lower Cretaceous from E to W indicates Mesozoic growth of the Tidsi anticline [5].

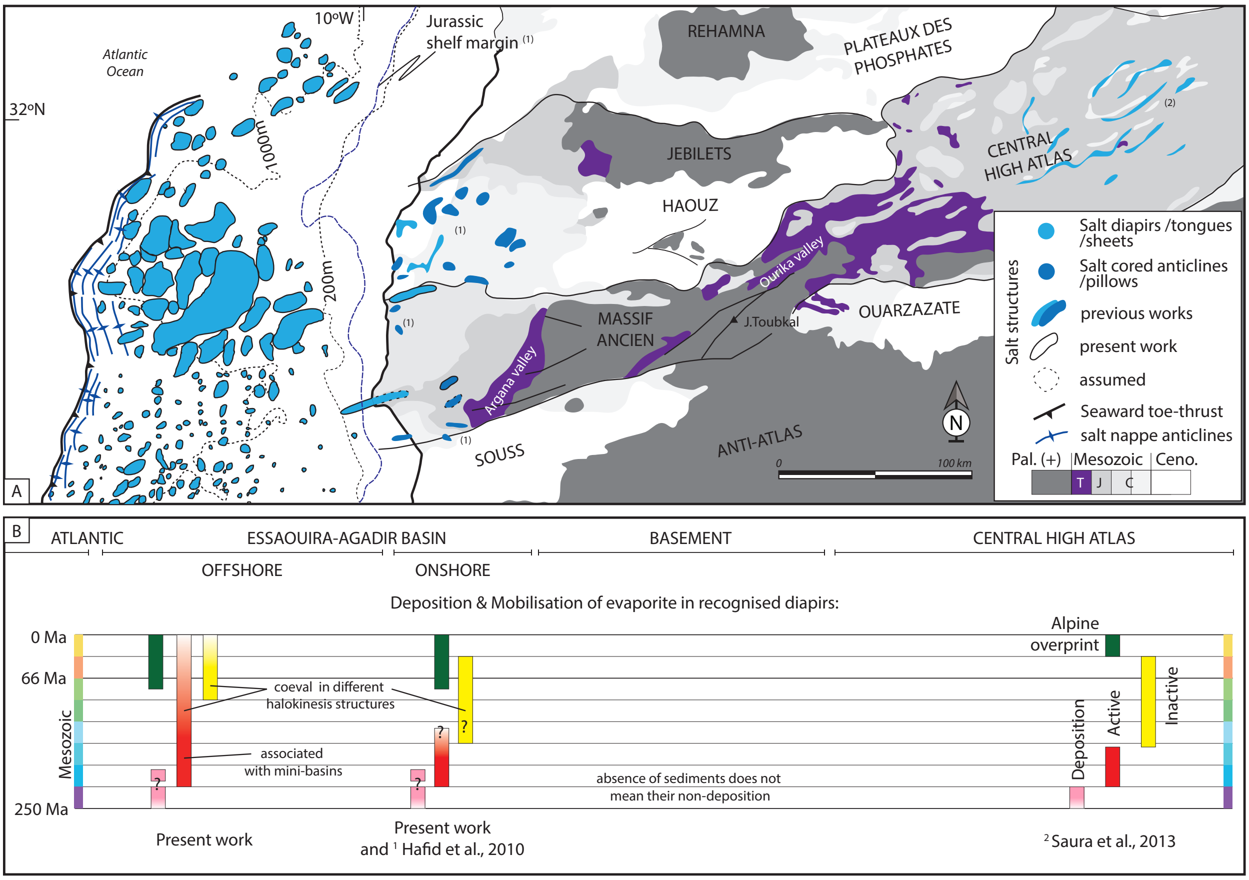

Figure 34: *Comparism of salt diapir activities in the Essaouira-Agadir basin offshore, the Western High Atlas onshore and the Central High Atlas (in cooperation & with permission from Leonardo Munizpichel (NARG), Aude Duval-Arnould (NARG) & Rémi Charton (NARG)).*

6.1.3 Salt Diapir Mechanics

Salt tectonics are a pressure-driven and gravity induced phenomena, in which salt flows from low to high pressure areas depending on variations in the thickness, density, or strength of overburden strata above salt [23], [24]. Evidence for Middle Jurassic active salt diapirism were found in both anticlines. The thickness and age of the salt in the Imouzzer (Lower Lias) and Amsittene (Upper Triassic) might be different, but the processes and timing of mobilising the salt bodies are somewhat similar, suggesting that they are even connected. The Lower Liassic salts seem to be relatively thin and interbedded in carbonate layers, which goes along with the observations of thin salts causing structures dominated by thrusts and narrow box-fold anticlines [23]. The present day salt deformations observed in the Imouzzer anticline, show no major orientation of deformation, but are relatively chaotic in orientation and deformation patterns, suggesting early salt diapirism independent of a clear N-S compressional component. Both salt horizons were possibly active from Early to Middle Jurassic, creating sediment thinning, extensional deformational features and crestal erosion. Still, it remains difficult to determine the processes causing the salt to mobilise.

Three types of loading can drive salt flow: (1) gravitational loading, (2) displacement loading and (3) thermal loading [23] (fig. 35). The gravitational loading theory (1) is based on the concept of a hydraulic head gradient, initiated by a combination of the weight of rocks overlying the salt and the gravitational body forces within the salt [23]. The total hydraulic head is the elevation of a particle of fluid above some arbitrary horizontal datum, whereas the pressure head is the height of a fluid column that could be supported by the pressure exerted by the overlying rock. Considering the Jurassic vertical movements in the passive margin of Morocco, the Moroccan hinterland was exhumed in the Jurassic [17], [19], [40], whilst the WHA shows subsidence [5], [18]. This can create a slope and a hydraulic head by gravitational loading, leading to the initiation of lateral salt flow and consequent folding in the WHA (fig. 35). However, sediment thicknesses along this transect control the mode of functioning: 1a) The exhumation is leading to erosion and down-shedding of sediments from E-W creating a thickening towards the east ($t_1 > t_2$) and consequent salt flow towards the west. 1b) Sediment thickness is constant or very small ($t_1 = t_2$), but the salt in the east of the basin is affected by the exhumation, leading to salt flow towards the west. 1c) Sediments are thicker in the west ($t_1 < t_2$, but $z_1 > t_2$), typical for rift basins associated with normal faulting and tilted fault blocks. Zühlke *et al.* (2004) described a general thickening of Jurassic successions from the north-east towards the south-west from almost zero to about 800-1000m along a section from the Argana valley to the Late Jurassic continental shelf break [47], similar to what was measured in this project. Cretaceous rocks thicken from around 750m to 2500m. Therefore, a slope was likely present in Jurassic and Cretaceous times. Further, it rules out scenario 1a) because of the inverse thickness distribution and 1b) because thickness variations are generally present. In conclusion, scenario 1c) is most likely, suggesting an E-W orientated slope and consequent westward thickening, that might have lead to the lateral and asymmetric salt diapirism observed in the folds.

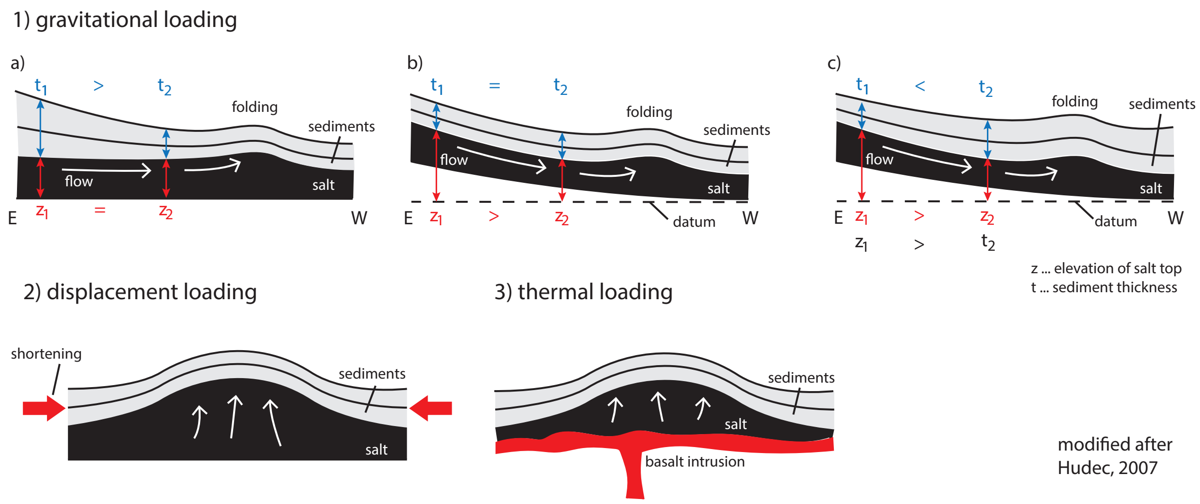

Figure 35: *Tentative models of salt diapir mechanics in the WHA (after Hudec, 2007).*

Another concept of salt diapirism is the displacement loading (2), in which shortening or extension leads to the initiation of folding above weaker salt layers, independent of regional thickness variations [23]. Such a tectonic component, for example regional shortening, was previously discussed [5], [34], [40]. Further, roofs more than several hundred meters thick are unlikely to be deformed by salt without the assistance from either regional extension or shortening [23]. A third option is salt mobilisation by thermal loading (3) at which hot salt expands and becomes buoyant, producing intrasalt convection [23] or inception of plug movements by igneous activity [8]. A heat source in the Late Triassic is the extensive magmatic activity (CAMP) forming large sheet basalts intercalated in large amounts of Late Triassic salts [20], [21], [42]. Salt heating and mobilisation in that case, must have occurred during the Late Triassic to Early Jurassic, when basalt intrusions were active providing the necessary heat (197-208 Ma).

From the study it seems likely that diapirism already occurred before commonly known episodes of regional shortening, i.e. the Alpine orogeny. Still, from the Alpine orogeny overprinted the fold structures from the Late Cretaceous, making the basin an inverted rift basin. Laterally shortened salt structures are often found in inverted rift basins and at the downdip toes of passive margins [26], [36]. Lateral shortening leads to the nucleation of folds and lateral fold propagation, linking pre-existing diapirs and commonly producing trends oblique to the regional shortening direction [23]. The position of outcropping salt and areas of thin sediments in the Amsittene and Imouzzer anticlines, probably caused by salt emplacement, seem to be at different positions along the fold. The Imouzzer anticline is also oblique to the generally N-S shortening direction of the Alpine orogeny, suggesting that the Alpine folding process is possibly driven by connecting pre-existing diapirs in the area. A similar situation is given in the Amsittene anticline, where indications for single, maybe even detached, salt diapirs are present in the Western part (salt mine) and the Eastern part, where sediments are clearly thinning and overturning of sediments in the Northern flanks disappears (fig. 17). Another theory is the impact on basement faults on salt diapirism and consequent folding mechanism. Hafid *et al.* (2000), debated the importance of basement faults, as they were reactivated during periods of extension and shortening [20]. The NNE-SSW to NE-SW trending reactivated normal fault systems [37] might have also defined the orientation and onset of salt diapirism, similar to what was described for the offshore areas [32].

6.1.4 Thickness Variations as Controlling Factor on Fold Belts

Assuming that Late Cretaceous to Neogene Alpine shortening led to compression and folding in the basin, thickness distributions of sediments can play an important role in basins as they can control the position, geometry and amplitude of such folds, comparable to the deformation in fold thrust-belts and thrust wedges.

The geometry of deformed basins, such as fold thrust-belts and thrust wedges, was described by different authors in the past. They describe different factors that control the evolution and geometry of those belts mainly in sand-box experiments and apply their observations on large-scale mountain belts. The variety of control parameters are sediment thickness, sedimentation rate, rock mechanical parameters, detachment surface, faults and most likely the slip tendency of a fault [27]. Marshak & Wilkerson (1992) find in their experiments that the wedge width is linearly dependent on sediment thickness and that this relation reflects the cross-sectional area balance in context of critical-taper theory: a given shortening of a thick sand layer must yield a wider wedge than the same shortening of a thin sand-layer [28]. Macedo & Marshak (1999) studied the geometry, specifically the curvature, of a large number of orogens and also concluded that the sediment thickness as a large controlling factor [27]. They showed that thicker basins accommodate more deformation than thinner basins, leading to convex shaped fold-thrust belts at pre-collisional depocenters. Storti & McClay (1995) studied the effect of syntectonic sedimentation on thrust wedges and found that the increasing sediment thickness reduces the lateral and vertical extent of the wedges due to an increase in normal stress [41]. Previous works addressed the role of small-scale field-geological features such as parasiteric folding, internal strain, small-scale faulting and fracturing on sediment thickness changes across a fold [2]. Still, there is no publication focusing on pre-tectonic thickness variations along-strike a folding structure. However, the mechanisms for thrust-fold belt and simple fold belt evolution are probably very similar. Assuming that no faulting is involved in the folding process and that the stress is constant and equal along the structure, the geometry can be assumed to be only dependent on sediment thickness, geomechanical parameters and sedimentation rate. This implies that the location, geometry and height of a simple fold structure are dependent on pre-deformational sediment depocenters and can therefore give indications about the basin evolution. Especially the plunging of a fold in a specific direction could be explained by sedimentary thinning towards the East.

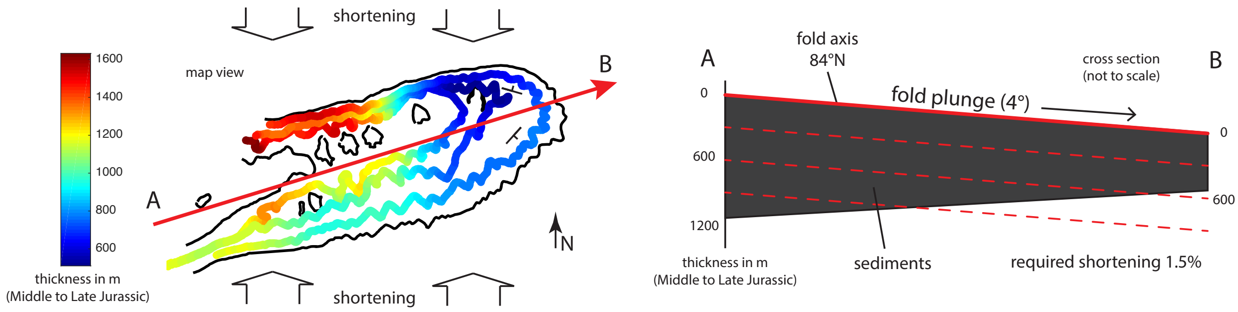

Figure 36: *Thickness variations in the Amsittene anticline affecting fold location, amplitude, plunge.*

Thickness distributions in the Amsittene anticline modeled in a 3D *Gocad* environment show deposition rates at different times of the Jurassic, as well as the geometrical structure of sedimentary layers. Clearly, the anticline is much thinner (up to 75%) in the eastern part compared to the middle part (fig. 36). This is especially noticeable in the Oxfordian and Callovian. The reason for the thickness difference may be related to salt moving upwards, creating depocenters and areas of low sediment thickness. The fold plunges gently about 4° towards the WNW, parallel to the observed orientation of sediment thinning. This results in a required tectonic E-W shortening of around 1.5%, which is a higher value than the one calculated from *Move* (less than 1%). Strain maps of the anticline indicate an elevated strain in the middle part and decreasing values towards the east, where the fold disappears. Elevated strain indicates increased folding activity, similar to what is suggested in fold-thrust belts with differential thickness distributions. Finally, the observed thickness changes might have influenced the location, amplitude and plunging style of the anticline during the N-S Alpine shortening event, similar to what was debated already for fold thrust-belts (fig. 36).

6.2 Source to Sink Sedimentation

The Western Atlas system, including the High Atlas, the Western High Atlas and the Agadir basin offshore are three systems forming a classical source to sink system with erosion in the Massif Ancien or HA due to periods of exhumation and uplift [40], sediment transportation in the WHA and finally deposition in the offshore basin. Middle Jurassic sedimentary transport directions in the WHA generally pointed westwards [1], [40], depositing large submarine fans in the offshore basin of the Atlantic ocean. The deposition is likely to be controlled by elevated areas and folds in the WHA basin, channelising sediments and controlling the locations of sediment deposition. Therefore, it is crucial to understand the timing of folds, such as the Amsittene and Imouzzer anticlines, to explain their role in controlling sediment distribution.

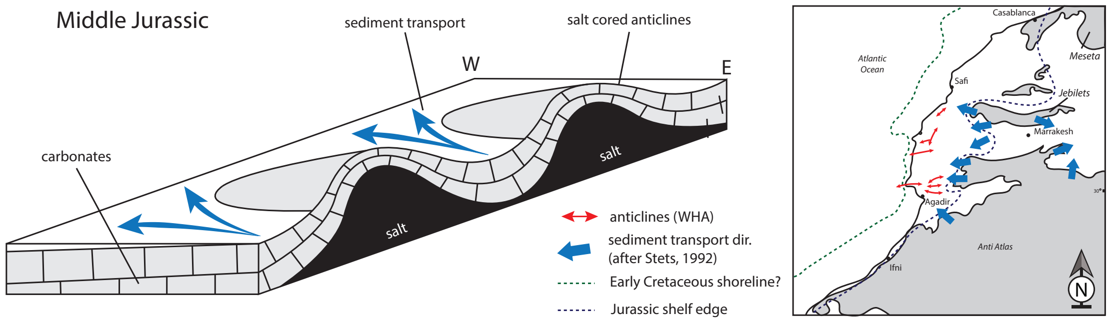

Figure 37: *Sediment transport pathways controlled by Middle Jurassic folding.*

Early to Middle Jurassic salt diapirism forming anticlines were proven by field observations, as well as 2D and 3D modeling results. Although the dimensions of salt induced fold growth are difficult to determine, they were presumably high enough to form Jurassic anticlines controlling the sediment transport in the area.

Structural data was obtained from only two anticlines, more anticlines of similar morphology exist in the basin, namely the Cap Rhir, Anklout and Lgouz anticlines. Assuming they all formed topographic highs already in the Early to Middle Jurassic, which remains to be proven, they certainly channelised sediments through the synclines in between (fig. 37).

7 Conclusions

This study shed new light into the controversially discussed question about whether salt-cored folds in the WHA are either shaped by compressional forces or salt diapirsm. The results show that salt mobilisation was a phenomena that was already active during the Early to Middle Jurassic and, therefore, before the Alpine orogeny starting in the Late Cretaceous. Thickness maps revealed the early deformation and localisation of depocenters in the Lias to Dogger. 2D unfolding and 3D strain analysis gave further evidence for pre-Alpine salt diapirism. Small scale field observations revealed different features indicating Jurassic syn-sedimentary features in both anticlines also confirming this theory. Mobilisation of Triassic and Liassic salt was most likely initiated by Jurassic exhumation patterns in the hinterland and subsidence towards the offshore, causing a hydraulic head gradient that led to lateral salt flow. Another possible scenario is a period of regional shortening in the Jurassic, similar to what was postulated in previous studies, but no direct cause of compression was found. As a consequence of early fold growth, the anticlines controlled the sediment pathways of eroded material coming from the exhumed Paleozoic massifs in the hinterland being shed towards the offshore basins. The location of deep-sea fans and clastic reservoirs of the Jurassic to Early Cretaceous are therefore dependent on the location of folds in the WHA. The early formation of salt domes and small diapirs possibly had a strong influence on the Alpine folding processes, such as: (1) pre-existing salt domes or diapirs defined weakness zones in the stratigraphic sequence which controlled the formation and location of Alpine folds and, (2) isolated, smaller salt domes or diapirs were connected during the Alpine orogreny, leading to the variety of strikes observed in most anticlines in the WHA; and (3) along-strike thickness variations influencing the location, amplitude and strain locations in folds.

For future projects, it is recommended to apply the same methodology to similar anticlines in the basin, namely the Tidsi, Cap Rhir, Anklout and Lgouz anticline, to compare the results. When obtaining elevation data for these models, other available sources, such as LiDAR, might give better results. Additionally, more field work is recommended to prove the suggestions that were provided from the modeling results. Syn-sedimentary deformation structures are likely to be found in areas where high strain values were calculated. Shallow seismic surveys perpendicular to the strike of the fold could add information about the thickness distributions away from the folds and could further shed some light on the connectivity of Triassic and Liassic salt bodies.

References

[1] R. Ambroggi. Étude géologique du versant méridional du haut atlas occidental et de la plaine du souss. Technical report, Royaume du Maroc, Ministère du Commerce , de L'industrie, des Mines et de la Marine Merchande, 1963.

[2] P. K. Atkinson and W. K. Wallace. Competent unit thickness variation in detachment folds in the northeastern brooks range, alaska: geometric analysis and a conceptual model. *Journal of Structural Geology*, 25(10):1751–1771, October 2003.

[3] M. L. Balestrieri, G. Moratti, G. Bigazzi, and A. Algouti. Neogene exhumation of the marrakech high atlas (morocco) recorded by apatite fission-track analysis. *Terra Nova*, 21(2):75–82, April 2009.

[4] G. Bennison and K. Moseley. *Geological Structures and Maps*. Hodder Education, 7th edition, 2003.

[5] G. Bertotti and M. Gouiza. Post-rift vertical movements and horizontal deformations in the eastern margin of the central atlantic: Middle jurassic to early cretaceous evolution of morocco. *Int J Earth Sci (Geol Rundsch)*, 101(2151-2165), 2012.

[6] K. Brautigam, D. Fernández-Blanco, and J. M. Klaver. Late jurassicearly cretaceous horizontal tectonics drives the jbel amsittene anticline in the haha basin, morocco. Master's thesis, Free University Amsterdam Free University of Amsterdam, Faculty of Earth and Life Sciences, 2009.

[7] R. Brown. Triassic rocks of the argana valley, southern morocco, and their regional structural implications. *The American Association of Petroleum Geologists Bulletin*, 64(7):988–1003, 1980.

[8] J. Callot, S. Jahani, and J. Letouzey. *The Role of Pre-Existing Diapirs in Fold and Thrust Belt Development*, chapter 16, pages 1–17. -, 2007.

[9] G. Caumon, G. Gray, C. Antoine, and M.-O. Titeux. 3d inplicit stratigraphic model building from remote sensing data on tetrahedral mehses: theory and applicaiton to a regional model of la popa basin, ne mexico. *Geoscience and Remote Sensing*, 2012.

[10] M. G. Choubert. Carte géologique du maroc - marrakech - 1/500000. Technical report, Ministére de L'energie et des Mines, 1957.

[11] D. F. de Lamotte, P. Leturmy, Y. Missenard, S. Khomsi, G. Ruiz, O. Saddiqi, F. Guillocheau, and A. Michard. Mesozoic and cenozoic vertical movements in the atlas system (algeria, morocco, tunisia): An overview. *Tectonophysics*, 475:9–28, 2009.

[12] P. Durand-Riard and G. Caumon, editors. *Balanced restoration of geological volumes with relaxed meshing constraints*. 29th Gocad Meeting, 2009.

[13] A. Ellero, G. Ottria, M. Malusà, and H. Ouanaimi. Structural geological analysis of the high atlas (morocco): Evidences of a transpressional fold-thrust belt. Technical report, Intech, 2012.

[14] N. Ellouz, M. Patriat, J. Gaulier, R. Buoatmani, and S. Sabounji. From rifting to alpine inversion: Mesozoic and cenozoic subsidence history of some moroccan basins. *Sedimenatry Geology*, 156:185–212, 2003.

[15] M. A. Fahmi, A. Plesch, J. Shaw, and J. Cole. Evolution of structures above a salt diapir - case study from the arabian gulf region. *AAPG Annual Convention and Exhibition*, May 2013.

[16] O. Fernandez, S. Jones, N. Armstrong, G. Johnson, A. Ravaglia, and J. Muñoz. Automated tools within workflows for 3d strucutral construction from surface and subsurface data. *Geoinformatica*, 13:291–304, 2009.

[17] B. Ghorbal. *Mesozoic to Quarternary Thermo-Tectonic Evolution of Morocco (NW Africa)*. PhD thesis, Vrije Universiteit Amsterdam, 2009.

[18] M. Gouiza, G. Bertotti, M. Hafid, and S. Cloetingh. Kinematic and thermal evolution of the moroccan rifted continental margin: Doukkalahigh atlas transect. *TECTONICS*, 29(TC5008):1–22, 2010.

[19] M. Gouiza, R. Charton, G. Bertotti, P. Andriessen, and J. E. A. Storms. Postvariscan evolution of the antiatlas belt of morocco constrained from lowtemperature geochronology. *Int J Earth Sci (Geol Rundsch)*, pages 1–24, 2016.

[20] M. Hafid. Triassic-early liassic extensional systems and their tertiary inversion, essaouira basin (morocco). *Marine and Petroleum Geology*, 17:409–429, 2000.

[21] M. Hafid, M. Zizi, A. W. Bally, and A. A. Salem. Structural style of the western onshore and offshore termination of the high atlas, morocco. *Geoscience*, 338:50–64, 2006.

[22] E. Hoffmann and F. Winde. Generating high-resolution digital elevation models for wetland research using google earth imagery - an example from south africa. *Water SA*, 36, 2010.

[23] M. R. Hudec and M. P. A. Jackson. Terra infirma: Understanding salt tectonics. *Earth-Science Reviews*, 82:1–28, 2007.

[24] M. P. A. Jackson. Retrospective salt tectonics. *Salt tectonics: a global perspective: AAPG Memoir*, 65:1–28, 1995.

[25] S. E. M. Jaidi, A. Bencheqroun, and M. Diouri. Carte du maroc 1/100000. In *TAMANAR*. Ministere du commerce, de l'industrie, des mines et de la marine marchande, direction des mines et de la géologie, 1970.

[26] J. L. B. C. J. Letouzey, J. C. Chermette, B. Colletta, and R. Vially. Evolution of salt-related structures in compressional settings. *Salt tectonics: a global perspective: AAPG Memoir*, 65:41–60, 1995.

[27] J. Macedo and S. Marshak. Controls of the geometry of fold-thrust belt salients. *GSA Bulletin*, 111(12):1808–1822, December 1999.

[28] S. Marshak and M. S. Wilkerson. Effect of overburden thickness on thrust belt geometry and development. *Tectonics*, 11(3):560–566, June 1992.

[29] A. Michard. *Continental Evolution: The Geology of Morocco*. Springer, 2008.

[30] Y. Missenard, Z. Taki, D. F. de Lamotte, M. Benammi, M. Hafid, P. Leturmy, and M. Sébrier. Tectonic styles in the marrakesh high atlas (morocco): The role of heritage and mechanical stratigraphy. *Journal of African Earth Sciences*, 48:247–266, July 2007.

[31] I. Moretti. Working in complex areas: New restoration workflow based on quality control, 2d and 3d restorations. *Marine and Petroleum Geology*, 25:205–218, 2008.

[32] M. Neumaier, S. Back, R. Littke, P. A. Kukla, M. Schnabel, and C. Reichert. Late cretaceous to cenozoic geodynamic evolution of the atlantic margin offshore essaouira (morocco). *Basin Research*, (1-19), 2015.

[33] C. Ogba and J. Richard. Analysis of accuracy of differential global positioning sytstem (dgps) and google earth digital terrain model (dtm) data using geographic information system technigues. In *FIG Working Week 2016*, 2016.

[34] A. Pique, P. L. Roy, and M. Amrhar. Transtensive synsedimentary tectonics associated with ocean opening: the essaouira–agadir segment of the moroccan atlantic margin. *Journal of the Geological Society*, 155:913–928, 1998.

[35] A. Piqué, P. Tricart, R. Guiraud, E. Laville, S. Bouaziz, M. Amrhar, and R. A. Ouali. The mesozoic-cenozoic atlas belt (north africa): an overview. *Geodinamica Acta*, 15:185–202, 2002.

[36] M. G. Rowan, F. J. Peel, and B. C. Vendeville. Gravity-driven fold belts on passive margins. *Thrust tectonics and hydrocarbon systems: AAPG Memoir*, 82(157-182), 2004.

[37] P. L. Roy and A. Pique. Triassic–liassic western moroccan synrift basins in relation to the central atlantic opening. *Marine geology*, 172(3-4):359–381, February 2001.

[38] N. Rusli, M. R. Majid, and A. H. M. Din. Google earth's derived digital elevation model: A comparative assessment with aster and srtm data. *Earth and Environmental Science*, 18, 2014.

[39] E. Saura, J. Vergés, J. D. Martín-Martín, G. Messager, M. Moragas, P. Razin, C. Grélaud, R. Joussiaume, M. Malaval, S. Homke, and D. W. Hunt. Syn- to post-rift diapirism and minibasins of the central high atlas (morocco): the changing face of a mountain belt. *Journal of the Geological Society*, 2014.

[40] J. Stets. Mid-jurassic events in the western high atlas (morocco). *Geologische Rundschau*, 81(1):69–84, 1992.

[41] F. Storti and K. McClay. Influence of syntectonic sedimentation on thrust wedges in analogue models. *Geology*, 23(11):999–1002, 1995.

[42] G. Tari and H. Jabour. Salt tectonics along the atlantic margin of morocco. *Geological Society of London*, March 2013.

[43] G. Tari, J. Monlar, P. Ashton, and R. Hedley. Salt tectonics in the atlantic margin of morocco. *The Leading Edge*, October 2000.

[44] F. Taylor. Nasa/japan release terrain data – google earth's is better.

[45] A. Teixell, M.-L. Arboleya, M. Julivert, and M. Charroud. Tectonic shortening and topography in the central high atlas (morocco). *Tectonics*, 22(5), 2003.

[46] P. van den Bogaard. The origin of the canary island seamount province - new ages of old seamounts. *Scientific Reports*, 3, 2013.

[47] R. Zühlke, M.-S. Bouaouda, B. Ouajhain, T. Bechstädt, and R. Leinfelder. Quantitative meso-/cenozoic development of the eastern central atlantic continental shelf, western high atlas, morocco. *Marine and Petroleum Geology*, 21:225–276, 2004.